Copyright Warning & Restrictions

The copyright law of the United States (Title 17, United States Code) governs the making of photocopies or other reproductions of copyrighted material.

Under certain conditions specified in the law, libraries and archives are authorized to furnish a photocopy or other reproduction. One of these specified conditions is that the photocopy or reproduction is not to be "used for any purpose other than private study, scholarship, or research." If a, user makes a request for, or later uses, a photocopy or reproduction for purposes in excess of "fair use" that user may be liable for copyright infringement,

This institution reserves the right to refuse to accept a copying order if, in its judgment, fulfillment of the order would involve violation of copyright law.

Please Note: The author retains the copyright while the New Jersey Institute of Technology reserves the right to distribute this thesis or dissertation

Printing note: If you do not wish to print this page, then select "Pages from: first page # to: last page #" on the print dialog screen

ABSTRACT

DIFFUSIVITY OF DRUG ACTIVES IN TRANSDERMAL DRUG DELIVERY (TDD)

by
Natali R. Gendelberg

Transdermal Drug Delivery (TDD) through skin patches has many advantages including the following: slow and continuous administration of the therapeutic over long periods of time, timely dosage, accessibility, kinetic maneuverability, elimination of the "First Pass Effect" and negative side effects on the digestive tract. All of the above justify investment into further development of TDD therapies, despite the skin permeability restrictions posed on size and charge by the skin. As skin permeability varies between all individuals based on age, ethnicity and lifestyle, the determination of the proper drug dosages to be contained in the skin patch is highly reliant on clinical trials. The objective of this research is to further investigate the application of components of a modified Duda-Zalinsky Equation (DZE) for drug diffusivity through a polymer matrix, to account for physical enhancers added to the Heated Lidocaine-Tetracaine Patch based on diffusivity results obtained from tests run in a Franz Cell apparatus. Pre-clinical trials computational estimation of the drug's diffusion properties with respect to the polymer matrix and skin will provide for safer clinical trials, with testing dosages that are closer to the therapeutic drug concentration in the blood.

DIFFUSIVITY OF DRUG ACTIVES IN TRANSDERMAL DRUG DELIVERY (TDD)

by
Natali R. Gendelberg

A Thesis
Submitted to the Faculty of
New Jersey Institute of Technology
in Partial Fulfillment of the Requirements for the Degree of
Master of Science in Materials Science and Engineering

Interdisciplinary Program in Materials Science and Engineering

May 2016

APPROVAL PAGE

DIFFUSIVITY OF DRUG ACTIVES IN TRANSDERMAL DRUG DELIVERY (TDD)

Natali R. Gendelberg

Dr. Nuggehalli M. Ravnindra, Thesis Advisor — Date
Professor, Department of Physics, NJIT
Director, Interdisciplinary Program in Materials Science and Engineering

---

Dr. Costas C. Gogos, Committee Member — Date
Distinguished Research Professor, Department of Chemical Engineering, NJIT
Principal Investigator, Polymer Processing Institute

Dr. Nikolas Ioannidis, Committee Member — Date
Research Engineer, Polymer Processing Institute

Dr. Michael Jaffe, Committee Member — Date
Research Professor, Department of Biomedical Engineering, NJIT

BIOGRAPHICAL SKETCH

Author: Natali Rachel Gendelberg

Degree: Master of Science

Date: May 2016

Undergraduate and Graduate Education:

- Master of Science in Materials Science and Engineering,
  New Jersey Institute of Technology, Newark, NJ, 2016

- Bachelor of Science in Biomedical Engineering,
  Rutgers College of Engineering, New Brunswick, NJ, 2012

Major: Materials Science and Engineering

Presentations and Publications:

Dana Knox Research Showcase, NJIT, Newark, NJ 4/20/2016
Poster Session – "Diffusivity of Drug Actives in Transdermal Drug Delivery (TDD)"
- Nominated for excellence by research advisor to present a poster on thesis research.

TMS 2016, 145th Annual Meeting & Exhibition, Nashville, TN 2/15/2016
Oral Presentation – "Transdermal Drug Delivery (TDD) Skin Patches"
- Was the opening speaker for the symposium title: Recent Developments in Biological, Structural and Functional Thin Films and Coatings – Biomedical and Energy Applications.

Afeka Academic College of Engineering, Tel-Aviv, Israel 1/10/2016
Presentation - "Noninvasive Computational Screening of Skin Patches"
- Gave a talk on the DZE equation, the Free-Volume Theory and its application to different skin patches and its potential in promoting novel developments.

המחקר הזה מוקדש לסבים והסבתות שלי ז״ל, אשר באומץ לב
נלחמו בתלאות חייהם על מנת שדורותיהם לעתיד ישגשגו ויחיו
בשלווה. הם ההשראה שלי, ואהבתם ונחישותם חסרת הגבולות
נותנת טעם לחיים ושמה אותם בפרספקטיבה. זכרונם
והמורשת שהשאירו אחריהם
מחזיקה אותי על הקרקע.

This Research is dedicated to my grandparents z”l,
who bravely fought through their arduous experiences
so that their future generations will peacefully thrive.
They are my inspiration and their love and limitless
unrelenting perseverance puts life into perspective.
Their memory and the legacy they have left behind
holds me down to earth.

ACKNOWLEDGEMENT

I would like to start by thanking my thesis advisor Dr. Nuggehalli M. Ravindra (Ravi) for his unwavering dedication and support throughout the entire research process. Ravi facilitated my research collaboration with Dr. Robert Falcone, who went out of his way to provide me with valuable advice and instructions that were crucial for my research.

I am also thankful for my thesis committee members for taking the time to serve on my thesis committee. Dr. Michael Jaffe is a long-time collaborator with Ravi's lab and it is always pleasant to hear his input. I first encountered Dr. Costas Gogos and Dr. Nikolaos Ioannidis in my Polymer Applications and Processing class, which became one of my favorite classes and topic of interest. Dr. Ioannidis was always very patient and helpful. Dr. Gogos is definitely one of a kind, with the breadth of his intelligence matching his heart of gold.

Galen US Inc. and their Medical Manager, Dr. Sarah Dolan have been an invaluable asset to my research. Sarah approved and arranged the donation of the Synera prescription topical patches for my investigation. Sarah was always nice and I do not have enough words to describe how thankful I am to her.

Another special contributor to my research, who I am very thankful for, is Mr. Yogesh Gandhi. He provided me with almost all of the equipment and reagents I needed and always offered more. I could always come to him for help knowing I will never receive a negative response. I am very thankful to Dr. Edward Dreyzin and Dr. Mirko Schoenitz for allowing me to make use of their TGA machine. Dr. Mirko Schoenitz deserves special thanks for running numerous TGA analyses for me and offering valuable input. Thanks to Dr. Russo and the Endomedix team for allowing me to use their facilities to perform the UV Spectrophotometric analysis. Bruce Slutsky has been absolutely

incredible throughout my research; he has been patient, kind and always went out of his way to provide personal dedicated assistance to provide all the library resources.

As Ravi refers to all of his students – “his family” – I have definitely witnessed it. Everyone is always willing to offer their help. I definitely appreciate all of the technical and emotional support I have received from Yan, Mostafa, Laxmi, Ruolei, Shuang, Scott, Asahel and Qian with whom I collaborated under the same research topic. Not many people know I have a few very valuable supporters from far away, whose love is very much felt despite the distance – thank you Dina, Efi, Gili, Stav and Jay for being part of my life.

I saved the best for last – my parents, brother and Scooby (our Pekingese). They are my supporting shoulder and will turn the world upside down just for me. They have always surrounded me with a lot of love, care and values. I appreciate them and love them. They give meaning to my life.

TABLE OF CONTENTS

TABLE OF CONTENTS
(Continued)

Chapter **Page**

LIST OF TABLES

LIST OF FIGURES

LIST OF FIGURES
(Continued)

CHAPTER 1

INTRODUCTION

1.1 Objective

The focus of this research is to examine a computational method for estimating the diffusivity of a drug diffusing through a polymer matrix, such as that found in a skin patch with additional physical diffusion enhancers. Components of a modified Duda-Zalinsky Equation (DZE) [1] for molecular diffusivity through a polymer matrix will be considered to assess the impact of a heat enhancement. The physical enhancement incorporated into the Synera Heated Lidocaine/Tetracaine patch (a local anesthetic manufactured by Galen Inc.) is considered within this context. The energy and viscosity values obtained computationally will be compared with diffusivity results obtained from tests performed on the patch in a Franz-Cell apparatus [2-10]. Such pre-clinical trials and computational analysis of the diffusion characteristics of the drug will allow for proper dosage of the skin patches, thereby reducing the risk involved in clinical trials.

1.2 Skin Anatomy

The skin is the largest organ in the human body, with the primary purpose of preventing the entrance of foreign invaders. Additionally, the skin serves as a tool for body temperature adjustment and for sensory purposes. The skin's three primary layers are, from top to bottom, the epidermis, dermis and hypodermis that mainly contains subcutaneous fatty tissue (Figure 1.1). The cells that make up the skin are called keratinocytes, due to

their increased production of the protein keratin that protects these epithelial cells from damage due to exterior stresses [11].

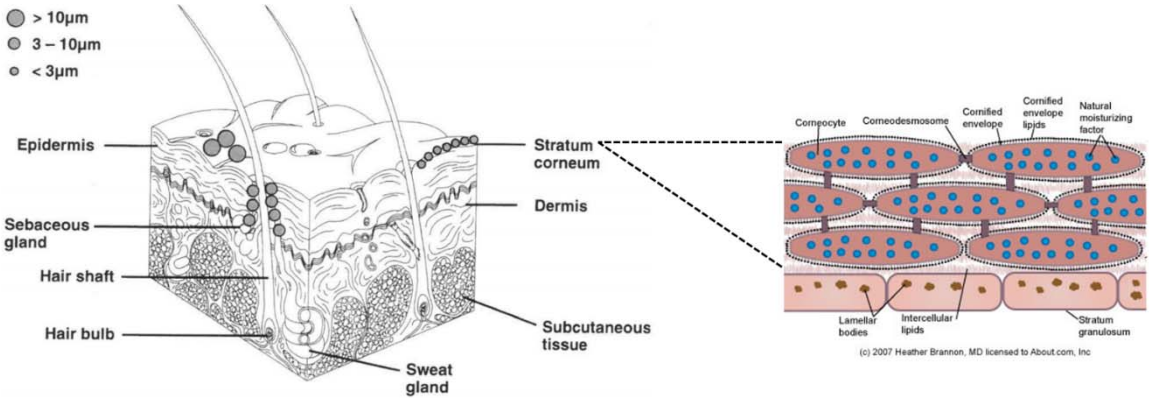

Figure 1.1 Skin anatomy with a close up of the SC and drug diffusion paths in the inset.
"Human Skin Anatomy Diagram." *Human Anatomy Body Picture*.
Benita S. *Submicron Emulsions in Drug Targeting and Delivery*.

The epidermis consists of the stratum corneum (SC), a pigment layer and at the interface with the stratum basale of the dermis – the stratum spinosum. The stratum spinosum consists of basal cells that interlock with the dermal papilla that stick out of the stratum basale. Sweat pores that allow for water evaporation for body temperature mediation can be found on the surface of the SC. Sweat glands are located in the hypodermis, but are connected to the sweat pores and extend through all skin layers. The hair shaft extends out of the SC from the hair follicle that extends into the hypodermis, with the papilla of the hair located in the hypodermis. Each hair follicle contains sebaceous glands on its side, which secrete oil into the hair follicle in order to prevent the hair shaft from becoming brittle [11].

The skin performs several sensory functions. The dermis holds nerve endings closer to the interface of the epidermis and the dermis and extend into the hypodermis, thus giving them sensitivity to touch on the surface of the skin. The Pacinian corpuscles are nerve receptors embedded in the hypodermis and detect pressure and vibration. Arrector pili

muscles attached to the hair follicles are controlled by the sympathetic nervous system to contract and further insulate the skin, which causes rising of the hair shaft. Dispersed nerve endings extending throughout skin layers, blood and lymph vessels (located in the hypodermis) and hair follicles serve to detect and amplify sensory response [11].

This research is primarily focused on the SC, as it is the rate limiting step in TDD diffusion. As can be seen in the inset in Figure 1.1, the SC has a "brick and mortar" infrastructure. This brick-like characteristic is due to the ordering of the corneocytes that are linked via corneodesmosones, while the mortar-like characteristic is due to the lipid medium in between the corneocytes. Corneocytes are "dead" keratinocytes that are filled with keratin and engulfed in a cornified envelope of lipids and surrounded by a lipid filler. This foundation of the SC allows for only two paths for drug diffusion: directly through the corneocytes and lipids or solely through the surrounding lipid paths. These conditions provide both charge and size restrictions on the penetrant. In order to diffuse through the SC, the drug must be neutral and must abide by the "500 Da Rule". The "500 Da Rule" is primarily based on clinical results and analysis of natural skin penetrants, which show that only molecular compounds or drugs with molecular weight less than 500 g/mol can freely diffuse through the SC [14].

1.3 TDD Market

The TDD market was valued at approximately $27 billion in 2013 and was predicted to experience an 8% Compound Annual Growth Rate (CAGR) for the five years following the publication of this report [16]. Local anesthetic patches have undergone several upgrades over the years, despite their constituting only 2% of the global TDD market

(Figure 1.2) [17]. Part of the interest in investment into local pain relief patches is to control usage of such therapeutics as they are controlled substances that may cause addiction. Furthermore, slow release patches are more effective than bolus doses that fluctuate.

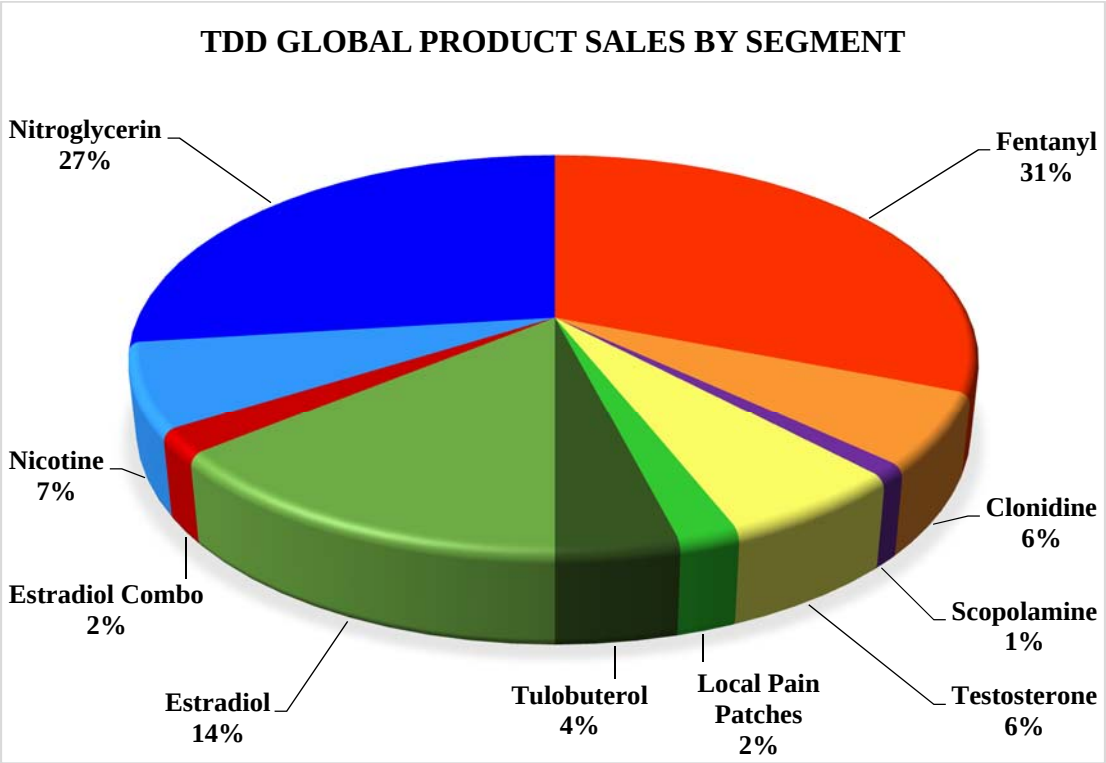

Figure 1.2 Global TDDS sales by segment.
B. Debjit, S. Duraivel, and K. P. .Sampath Kumar. "Recent Trends in Challenges and Opportunities in Transdermal Drug Delivery System." *The Pharma Innovation* 1.10 (2012): 9-23. Web.

Targeted drug delivery and sustained release drugs (Figure 1.3) are shown in the bar graph for market value of oral drugs. Sustained release drugs do not solely represent skin patches, which explains the increased value of the market sector, compared to the value reported in the previous paragraph. The key growth trends, observed in this depiction, between 2004-2011 are: a 2.5x increase for transmucosal drug delivery, a 5x increase for targeted drug delivery and a 1.8x increase for sustained release, implants and TDD. The former value can seem unnerving, compared to the increase in value associated with

targeted drug delivery. This drastic difference is due to several factors. First, targeted drug delivery technologies experienced a significant breakthrough between the years 2006-2011, before which sustained release, implants and TDD dominated the therapeutics market as its primary constituent. Second, sustained release, implants and TDD still encompass almost half of the therapeutics market. Third, many targeted drug delivery technologies utilize TDD and sustained drug release. Therefore, the extreme increase could be due to intermarket overlap. The increase in market value of transmucosal therapies does not signify a potential profit. The drug market percentage represented by transmucosal drugs decreased by 2% and began at a substantially lower value compared to other therapies.

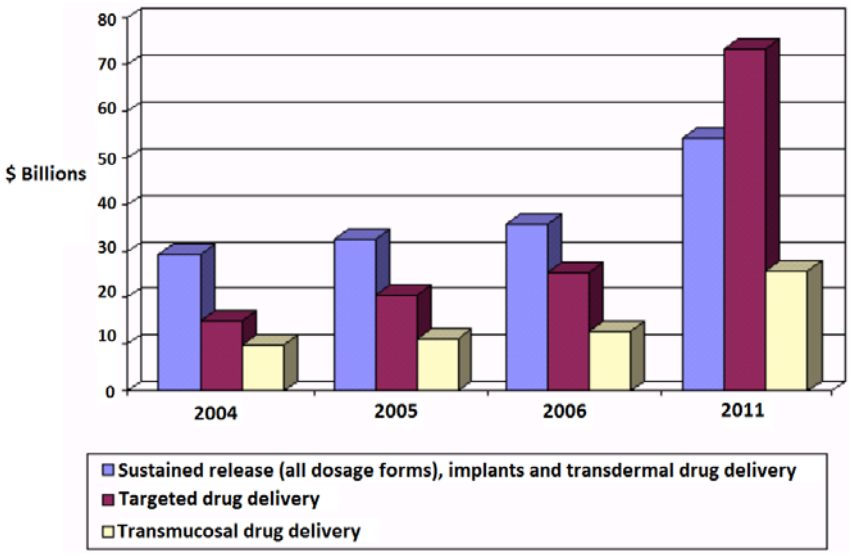

Figure 1.3 Drug delivery market trends.
S. Kumar, K. P., D. Bhowmik, B. Chiranjib, and R. M. Chandira. "Transdermal Drug Delivery System - A Novel Drug Delivery System and Its Market Scope and Opportunities." *International Journal of Pharma and Bio Sciences* 1.2 (2010): 1-21. Web.

1.4 Advantages of TDD

Transdermal drug delivery has a slow and continuous drug release profile. This sort of profile is ideal for treatments involving drugs with a short half-life that must be administered frequently over long periods of time. The patch's constant presence also ensures timely dosages that prevent unwanted variations in the drug's blood concentration.

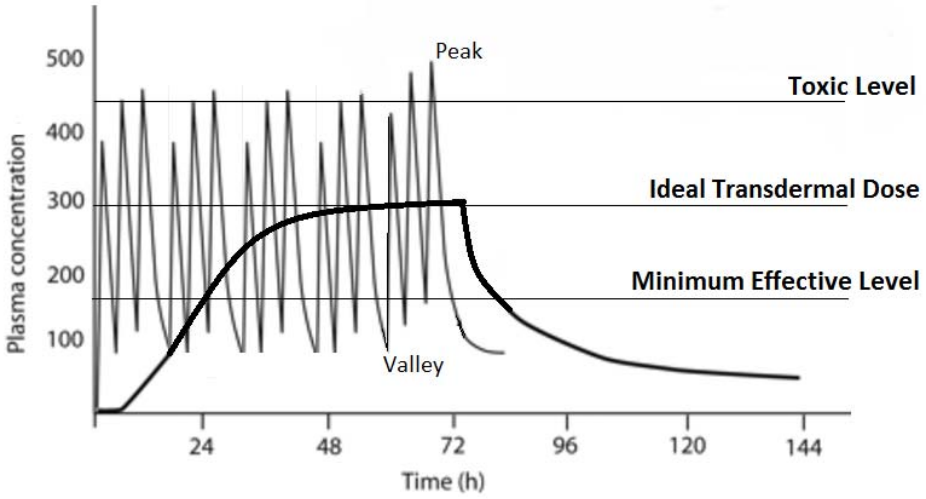

Figure 1.4 Cycle of blood concentration with respect to time in TDD.

The skin's large surface area makes skin patches a highly accessible, yet non-invasive and kinetically maneuverable form of treatment. As can be seen in Figure 1.4, oral and bolus drug administration involve fluctuations of the drug concentration in the blood, with a spike at the time of administration and a sudden decrease at peak concentration. In order to obtain an average dosage around the middle of the therapeutic range, the initial dosage must be much higher. Each valley-to-valley segment of Figure 1.4 represents a single administration. From this representation, it is evident that such treatment involves cyclical dosage fluctuations whose range varies between individuals based on weight, age, life-style and genetics. Therefore, for different individuals, the valleys and peaks of the

drug administration may exceed or fall below the toxic and minimal therapeutic drug concentrations, respectively [19].

The oral/bolus forms of drug administration set up a precedent where a patient is at risk or is not receiving effective treatment at a certain fixed time, which can also bring upon a set of side effects such as nausea. In contrast, the skin patch maintains a quite consistent dosage that can be tailored by modification of the polymer matrix through which the drug diffuses. Application time of the patch is determined based on the point at which the drug remaining in the patch reservoir provides for the determined margin of decrease in resulting blood concentration. Furthermore, administration can be instantaneously halted via patch removal in the case of evident deleterious side effects.

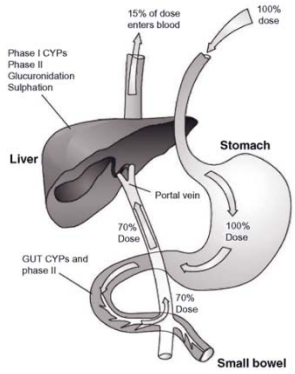

Figure 1.5 Illustration of the "First Pass Effect".
"First Pass and Plasma Drug Levels (Introduction) (Human Drug Metabolism)." *Whatwhenhow RSS*. Web. 03 Feb. 2016.

The ability of the skin patch to circumvent passage through the gastrointestinal tract (GIT) has two advantages: 1) the drug does not damage the GIT or its mucus membrane and 2) the "First Pass Effect" is eliminated. The "First Pass Effect" (Figure 1.5) is a result of the body's clearance system. After entering the stomach, the drug may be detected and cleared out by the body as a foreign object in passage through the intestines and the liver, resulting in a reduced dose entering the blood stream where the drug undergoes another

series of clearance. This requires that the initial dosage administered to the patient be much higher than the therapeutic dosage. As the amount of drug cleared out varies between individuals, as mentioned above, this may result in varying side effects that cannot be halted without complete clearance that is physiologically controlled [20].

1.5 Limitations of TDD

The skin's foundation is built on preventing the entrance of any foreign objects into the body. As such, the charge and size limitations, discussed in the skin anatomy section, eliminate the design of skin patches for a large scope of therapeutics, including: gene therapy, liposomal drug delivery and charged particles. As an individual's lifestyle impacts metabolic activity, while SC thickness and skin composition varies in different parts of the body and between individuals, the theoretical blood dosage with respect to polymer matrix design varies between individuals and is highly reliant on clinical trials. As a result, skin patch dosages are determined based on clinical trial results and thus pose high risk to the subject as the resulting dosage may fall in an individual's toxic dosage. Finally, skin adhesives may cause skin irritation and rash [1, 22].

CHAPTER 2

BACKGROUND

2.1 Basic Skin Patch Construct

The two primary types of skin patches are: the reservoir patch and the matrix patch (Figures 2.1 and 2.2, respectively). The main difference between these types of patches is their form of drug storage and kinetics. The patch acts as an initial drug reservoir. Once the patch is placed at the site of application, the drug begins to diffuse into the SC due to osmotic pressure and forms a secondary reservoir in the SC, which further emphasizes the SC's rate limiting property. The drug diffuses through the SC into capillaries, present in the hypodermis and thereby enters the blood stream [23].

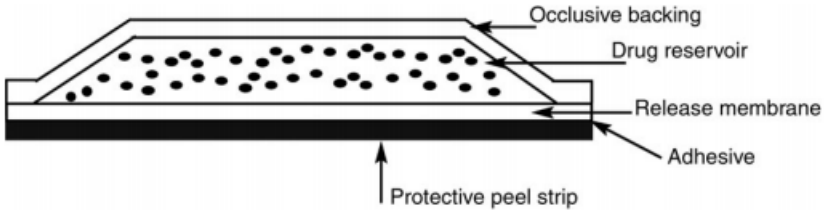

Figure 2.1 Cross-section through a reservoir patch.
Margetts L. and Sawyer R. "Transdermal Drug Delivery: Principles and Opioid Therapy." *Contin Educ Anaesth Crit Care Pain Continuing Education in Anaesthesia, Critical Care & Pain* 7.5 (2007): 171-76.

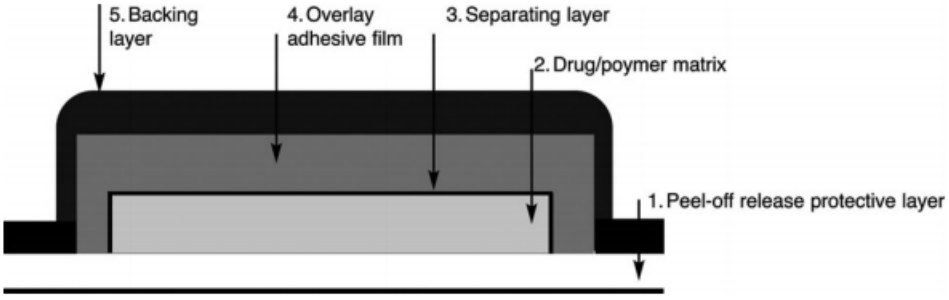

Figure 2.2 Cross-section through a matrix patch [23].
Margetts L. and Sawyer R. "Transdermal Drug Delivery: Principles and Opioid Therapy." *Contin Educ Anaesth Crit Care Pain Continuing Education in Anaesthesia, Critical Care & Pain* 7.5 (2007): 171-76.

The reservoir patch contains the drug in liquid form in a reservoir on top of a polymer membrane interface, which acts as the rate limiting component of drug release from the patch itself. This feature allows for greater control of the drug delivery rate by varying the polymer membrane composition, conformation and constituents. Despite the increased control over the diffusion rate, an initial burst of the drug may occur due to the large concentration difference between the drug reservoir and SC as the SC initially has yet to form its own drug reservoir. Furthermore, any inconsistency in the polymer membrane thickness may pose as a site of increased diffusion rate that may cause an overdose. In the matrix patch, the drug is evenly distributed in the adhesive polymer matrix, with the drug diffusion rate limiting factors being the amount of drug held in the polymer matrix, the formulation of the polymer matrix and the area of the patch applied to the skin [23].

2.2 Governing Diffusion Equations

Diffusion involves the movement of particles from regions of high concentration to regions of low concentration via random movement. Diffusion whose driving force is solely the concentration gradient between regions in the volume of diffusion is referred to as passive diffusion, with the movement of the diffusing particles following the "Random Walk" model or probability function. This type of diffusion is quite slow with a well-defined direction. In some cases, where diffusion must occur faster or against a concentration gradient (i.e., to trigger another process), a convective factor is added to the diffusion in the form of additional energy or physical barriers. In 1855, Adolf Fick derived the most basic governing diffusion equation [24].

$$J = -D\frac{dC}{dx} \tag{2.1}$$

The flux J represents the amount of particles diffusing through a cross sectional area perpendicular to the path of diffusion. Fick's First Law of Diffusion provides information on the expected amount of flux. Figure 2.3 shows that the flux is proportional to the diffusivity of the particle, D, which accounts for the tendency of the particle to diffuse through the medium. The concentration gradient, dC/dx, generates the energy that causes the particles to diffuse from areas of high concentration to areas of low concentration. The negative sign in equation (2.1) signifies the increase in flux in the direction of decreasing concentration [24].

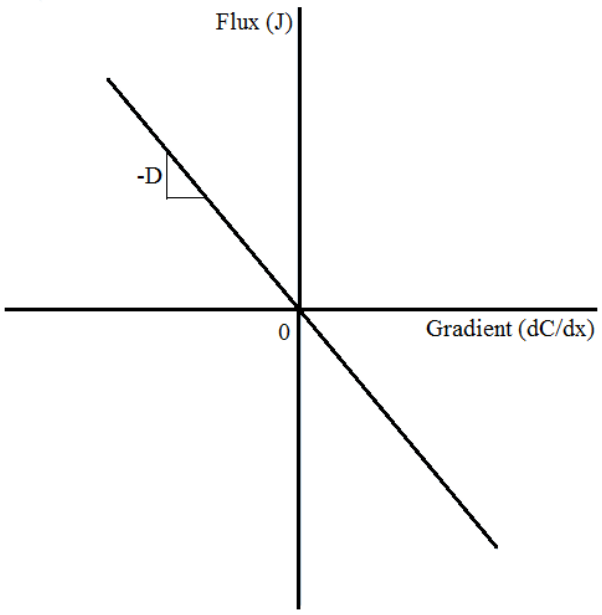

Figure 2.3 Fick's 1st Law plotted in terms of the flux with respect to the concentration gradient.

$$-\frac{\partial J}{\partial x} = \frac{\partial C}{\partial t} = \frac{\partial}{\partial x}\left(-D\frac{\partial C}{\partial x}\right)$$

$$\frac{\partial C}{\partial t} = D\frac{\partial^2 C}{\partial x^2} \tag{2.2}$$

Fick's Second Law of Diffusion (equation (2.2)) provides information regarding the rate of change of concentration at any point in space. The left side of the equation, the gradient of the concentration with respect to time, is directly related to the Laplacian of the concentration with respect to distance from the cross section through which the particles diffuse.

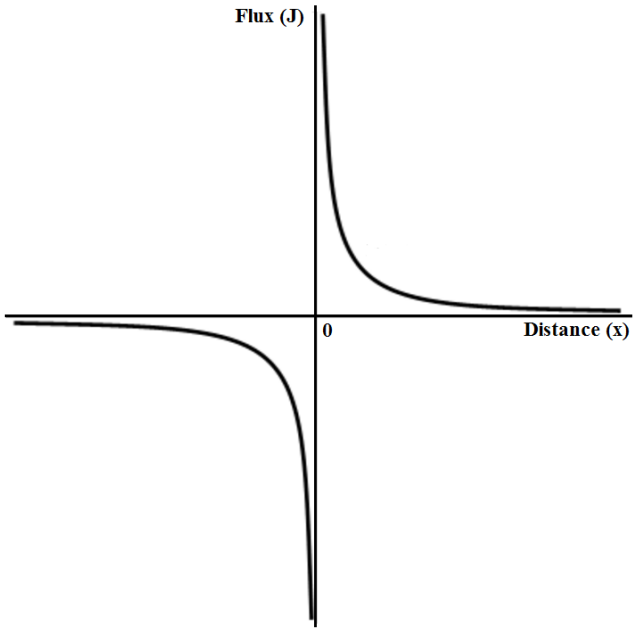

Figure 2.4 Fick's 2nd Law plotted in terms of the flux with respect to the distance from the cross sectional area perpendicular to the path of diffusion.

Figure 2.4 depicts this relationship in which the flux approaches zero with increasing distance from the cross sectional area being analyzed, regardless of the distance being in front or behind the cross sectional area. As the distance to the cross sectional area, perpendicular to the path of diffusion, approaches zero from the positive direction, the flux

goes to infinity. Conversely, as the distance to the cross sectional area, being discussed, is reduced in magnitude from the negative direction, the flux approaches negative infinity [24].

Steady-state diffusion is diffusion that is not time dependent. In contrast, nonsteady-state diffusion is time dependent and exhibits varying diffusion profiles at varying time points. Fick's second law of diffusion is primarily used for nonsteady-state diffusion profiles as it contains a time dependent term. In analysis of steady-state diffusion, the gradient of concentration with respect to time term is equal to zero.

2.3 Diffusion Through Skin

In order for diffusion to be feasible and predictable in a noninvasive manner, the drug's diffusivity needs to be estimated. The simplest calculation for molecular diffusivity is given by the Stokesian Diffusion, in which a spherical particle with radius *r* diffuses through a continuous fluid medium (equation (2.3)). The numerator of the Stokes-Einstein equation accounts for the positive contribution due to particle diffusion in terms of absolute temperature (T) and the Boltzmann constant (k), whereas the denominator emphasizes that increasing particle size (r) and viscosity (μ) poses a hindrance for diffusion. The viscosity plays a significant role because each individual particle gets engulfed by a static layer of the fluid medium. This results in a friction between the static layer and the fluid medium moving relative to the diffusing particle [25].

$$D_0 = \frac{kT}{6\pi\mu r} \tag{2.3}$$

Aside from the direct temperature correlation seen in equation 2.3, there is a hidden exponential temperature factor that contributes to the particle diffusivity that is hidden in the temperature dependence of viscosity. Evidence of this dependence is visible in equation (2.4), Joback's equation for viscosity, which correlates the liquid dynamic viscosity (μ_L, units: Pa·s) to the sum of constant viscosity factors per bond group in the molecule (μ_a and μ_b) and the temperature (T). The division of bond segments in the molecule refers to carboxyl bonds, double bonds, bonds that are part of an aromatic ring etc. This equation is valid between the melting temperature of the molecule and 0.7 times its critical temperature, i.e., the temperature at which the gas form of the molecule can no longer condense back into solution [25]. Viscosity decreases with temperature exponentially because more molecules obtain sufficient energy to overcome the resistive shearing forces that hinder diffusion or movement. Also, greater particle mobility results in a higher level of disorder that thins out the liquid. The Stokes-Einstein diffusivity does not consider particle shape; it contains two particle size factors – the radius in the denominator and the molecular weight in the viscosity calculation.

$$\mu_L = MW e^{\left[\frac{\sum \mu_a - 597.82}{T}\right] + \sum \mu_b - 11.202} \tag{2.4}$$

More often than not, the geometry of the particle diffusing or the nature of the medium results in Non-Stokesian Diffusion. Large particles that are arranged in chains or complex geometries, i.e., polymers, proteins etc., may change geometry as a result of the attractive forces between the medium and side groups, may have their center of gravity in a nonsymmetrical position along their length and may diffuse in different directions. This

results in more complex diffusion patterns that are dependent on the available free volume/holes that can accommodate the movement, geometry and molecular properties of the diffusing particles with respect to their matrix.

As the polymer membrane through which the drug active diffuses in the patch is not a fluid, the Stokes-Einstein parameters are breached. Furthermore, the cell membrane exhibits anisotropic diffusion/penetration properties. The fluid in the plane of the membrane results in transverse particle diffusion through the fluid. In one form of diffusion through the SC, lateral diffusion or transmembrane diffusion, the diffusing particle is set back by the hydrocarbon chains that are vertically anchored. In the second form of diffusion through the SC matrix (around the corneocytes), there are physical hindrances that lead to loss of energy to the particle and results in a smaller diffusivity. The "brick and mortar" structure of the SC prevents transmembrane diffusion and facilitates increased diffusion path length. Therefore, in both processes of diffusion through the skin patch membrane and the skin, the diffusion of the drug is Non-Stokesian [25].

Non-Stokesian diffusivity computations vary based on diffusion characteristics. They normally involve adding an exponential multiplier to the Stokes-Einstein equation that accounts for the system's deviation from Stokesian Diffusion. In the case of particles diffusing through a polymer membrane and the SC, analysis via the free volume theory is most adequate. This analysis involves an exponential factor that is a probability function that computes the probability of the diffusant encountering a hole with the minimum critical volume required for diffusion to occur. In this view, the particle and the hole are viewed as mutually diffusing.

Experiments performed to assess free hole volume in a hydrocarbon chain matrix, which can be compared to the hydrocarbon tails of the cell membrane, showed that approximately 35% of the total volume is attributed to free hole volume [26]. It is not feasible to computationally calculate the exact free hole volume in a polymer matrix as it accounts for the difference between the total volume of the matrix and the Van der Waals volume of the polymers, which may vary with time as well. Therefore, the free hole volume should be statistically based on the following premises: 1) it is most probable to encounter small holes and 2) the formation of large holes is highly improbable. Thus, the diffusion coefficient depends on the number of holes, the net hole formation frequency and the probability of finding a hole as a function of the exponent of the ratio of the minimum hole volume necessary for diffusion with respect to the average hole volume [25].

$$D_\infty = D_0 e^{-E/kT} e^{-\varepsilon V^*/V} \tag{2.5}$$

$$\varepsilon = \frac{\hat{V}_1}{\hat{V}_2}$$

The basic probability function for diffusion through a polymer matrix is that posed by Vrentas and Dudas for the infinite particle diffusivity, as can be seen in equation (2.5). The term D_0 refers to the Stokes-Einstein diffusivity (equation (2.3)). The first exponential term accounts for the Arrhenius factor of the diffusion that is related to the kinetic energy of the diffusing particle. This E term refers to the activation energy required for the drug to overcome the attractive intermolecular forces with its medium in order to diffuse. T refers to the temperature in Kelvin and k is the Boltzmann constant. The second exponential term accounts for the ratio of the critical jumping volume required for diffusion with

respect to the total available free volume (V^*/V) multiplied by the ratio of the solvent to polymer jumping unit that is determined by a factor of the occupied volume of the diffusing molecule (subscript 1) and the polymer matrix (subscript 2) [1]. Table 2.1 emphasizes the role of the shape of the diffusing molecule. It is evident that, for molecules of equal volumes, the elongated molecules have a greater diffusivity. This phenomena is attributed to the higher probability of the longer configuration of the molecule finding a hole that fits its smaller cross section (the cross sectional area perpendicular to its length). This directional diffusion property is referred to as reputation [25].

Table 2.1 Effect of the Shape of a Diffusing Molecule on Diffusion in a Polymer

Effect of the Shape of a Diffusing Molecule on Diffusion in a Polymer[a]

Diffusant	Diffusion Coefficient (D) $\times 10^9$ ($cm^2\ sec^{-1}$)
Propane	4.81
n-Butane	3.24
n-Pentane	2.64
n-Heptane	3.04
n-Octane	3.16
Isobutane	1.45
Isopentane	1.32
Neopentane	0.62

Stein, Wilfred D., and W. R. Lieb. *Transport and Diffusion across Cell Membranes*. Orlando: Academic, 1986, 94-102.

2.4 TDD Penetration Enhancement Technologies

The purpose of investment into TDD penetration enhancement technologies is to improve drug diffusion and to facilitate the utilization of TDD for a wider range of drugs, including those that violate the charge and size barriers posed by the SC. The two categories of these technologies are: physical penetration enhancers and physical methods of TDD. Physical penetration enhancers include modifications to the SC to increase its permeability or its electrochemical character, including: Iontophoresis, Electroporation and Ultrasound/Sonophoresis. Physical methods of TDD involve a more forceful circumvention of the SC that might involve its local elimination; such methods include: Hypodermic Needles, Jet Injections, Crystal Microdermabrasion, Thermal Ablasion, Laser Ablasion and Microneedles [27].

A schematic of the construct of an iontophoretic system is shown in Fig. 2.5. The system involved contains two electrodes that are in contact with the skin and extend out of electrolyte chambers. One electrolyte chamber contains the drug along with anions (if the drug is cationic, as in the figure), while the other chamber contains a buffer solution of similar polarity.

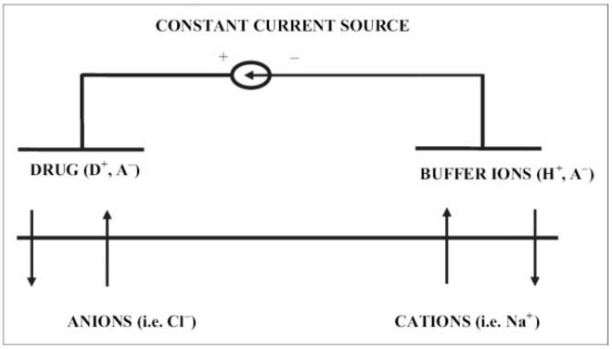

Figure 2.5 Depiction of an Iontophoretic electroosmotic system on the ionic level.
Bhowmik, D., Duraivel, S. and Sampath Kumar, K.P. "Recent Trends in Challenges and Opportunities in Transdermal Drug Delivery System." *The Pharma Innovation* 1.10 (2012): 9-23.

A small electric current passing through the electrodes causes an electrical potential across the skin. As this functions as an electroosmotic system, the solvent flows in the direction of the ion movement and transports the cationic drug molecules through the skin. The dosage results from the magnitude of the charge generated by the applied current. This method generates better diffusion outcomes with cationic drugs because the cell membrane potential is negative, with increase in cationic drug contribution to electroosmosis being directly proportional to the molecular weight of the drug. However, the skin's permselectivity can be modified via adjustment to the formulation's pH, thereby promoting diffusion in the direction of the anions and allowing this method to be applied to anionic drugs as well. Additionally, increased ion mobility is preferable for decreased period of current passage, as the electrolytes "compete" to a certain extent with the active agent as charge carriers [28].

Despite osmosis generally being a passive form of diffusion, iontophoresis involves convective diffusion as the therapeutics are repelled into the skin. This property results in additional functions such as physiological monitoring by attraction of water soluble molecules present in the interstitial fluid. Drug dosages can be fine-tuned to provide for pulsatile drug delivery profiles that may prevent the body from becoming tolerant to the therapeutic [27]. Iontophoresis requires strict current limitation to prevent erythema. This method is not cost effective and was recalled by the European Medicine Agency due to continuous fentanyl release resulting from corrosion products from the system components when the device was deactivated, as well [22].

In electroporation, high voltage pulses are applied for a short duration to specifically increase SC permeability in controlled areas, thereby increasing the possible

diffusant size. The high-voltage electrical pulses disrupt the brick-and-mortar structure of the SC, which physically increases its susceptibility for diffusion while causing electrophoretic movement of the diffusing particles. This method provides promising in vitro result when compared to other permeability enhancers, but in vivo skin toxicological studies have yet to be sufficiently surveyed [22].

Ultrasound/Sonophoresis involves application of low frequency ultrasound to a site of the SC to increase the percutaneous drug flux. The SC's infrastructure is interrupted with the formation of cavitational bubbles by the ultrasound's oscillations. Sonication devices can include additional features, such as real-time impedance feedback that provides control over the activation of sonication with respect to the relevant conductance level. Despite the ability to individually tailor this form of enhancement, it is not widely used as its effect in humans is not sufficiently clear [22].

Hypodermic Needles that extend directly into the dermis are one of the most commonly used physical methods of TDD, with the feature of delivering impermeating and unstable compounds. This is achievable because the hypodermic needle acts as a piston that applies quickly a high pressure force that administers a large bollus of the drug, at an instant [29]. The controlled and continuous drug release that is desirable in TDD systems can be obtained by placing indwelling catheters in the skin. This method perforates the skin, thus making it invasive and a site of infection. In concept, Jet Injections are similar to hypodermic needles as they use high-pressure accelerators that utilize helium to push through either solid or liquid particles through the skin in a piston action. The advantage of jet injections over hypodermic needles lies in their noninvasive property, but they cannot facilitate long term drug release. Microscale microneedles are also used in a similar

manner, but they are designed short enough to avoid excitation of nerve endings while penetrating through the SC. Solid microneedles are used prior to the application of a skin patch, as the holes created result in skin permeability increasing by four orders of magnitude. Coating of the microneedles with the therapeutic allows for direct delivery of the drug upon penetration of the microneedles [27].

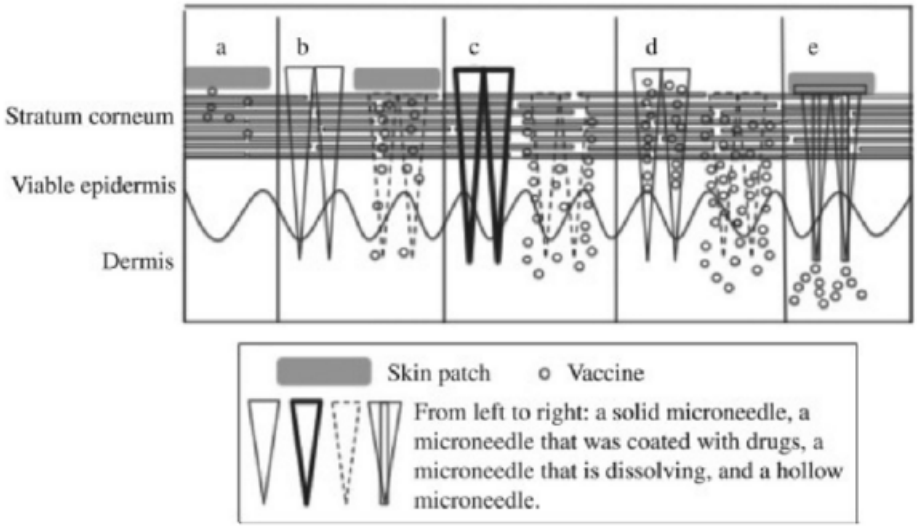

Figure 2.6 Sketch of different types of microneedles and their application.
Wang, Binghe, Longqin Hu, and Teruna Siahaan. *Drug Delivery: Principles and Applications*. 2nd ed. Wiley, 2005. Print. p. 217

Crystal microdermabrasion is a form of pretreatment to skin patch application. As part of the local preparation for application of the patch, the skin is exfoliated by microcrystals blown unto it. This treatment removes the CS, which has been shown to successfully increase the net flux and diffusivity of low-molecular weight drugs through the skin. Microdermabrasion is selectively designed to remove the SC only, while leaving the rest of the epidermis layer intact [27].

Laser ablation involves shining laser beams unto the skin to create pores through the SC that facilitate the diffusion of drugs that violate the charge and to some extent size limitations on TDD. This form of diffusion enhancement may also serve to extract

physiological data from the patient, by drawing interstitial fluid from the pores created in the SC. As laser ablation is a high-cost and complicated technology and this form of treatment is not for a single use, it is not widely used. This form of enhancement is not always performed a single time because the SC grows back and must be removed for subsequent patch therapies, which shows the advantageous minimally destructive character of this form of enhancement [22].

Thermal ablation works on the same premise as laser ablation, which is selective removal of the SC without causing permanent damage to the skin and its infrastructure. Heat is applied to the skin by an external heat source for a short amount of time, which disrupts and removes the SC and creates microchannel structures in the skin. The resulting microchannel structures are caused by three processes that occur as a result of the sharp heat exposure: (1) the loss of the structural viability of the brick-and-mortar structure of the SC; (2) the disruption of the keratin network within the SC; (3) the decomposition and vaporization of keratin due to heat, which leaves behind microscale vacancies in the SC [30].

It has been shown that the SC permeability is significantly increased with increasing temperature during thermal ablation, rather than with heating time. This being the case, there must be a strict control over the balance between effective temperature levels and exposure time of the tissue below the SC to prevent permanent damage to the skin. Lee et al. (2011) devised an apparatus to locally heat the skin for a duration of the order of 100 μs. This apparatus consists of water in a microchamber that is rapidly heated by discharging electric current through it. By utilizing the conversion of electrical current to thermal and mechanical energy in a localized manner, the generated jet of superheated steam is

immediately ejected unto the skin. In order to validate the effectiveness and safety of this construct, the authors [30] sought out to: (1) determine the heat transfer profile through the skin to produce a protocol with the most effective and safe heat level with respect to exposure time; (2) evaluate the efficacy of the microdevice in removing the SC, so as to improve skin permeability to hydrophilic molecules and macromolecules [30].

Thermal ablation was performed at a temperature of 1100 °C and tested for 1 μs, 10 μs, 100 μs, 1 ms, 10 ms and 100 ms time durations. Thermal ablation was tested for three levels of skin exposure: bare skin, skin covered by a heat conducting mask and skin covered by a heat conducting mask covered by a window patterned insulating mask. The skin exposed under latter conditions creates a perforated pattern on the SC, thereby showing precision of localization of the thermal ablation process while leaving segments of viable SC between the pores that can prevent infection and damage to future development of the skin. The 100 μs ablation time provided for the best combination of skin viability and increased permeability. The tested skin exhibited an increase of four and three orders of magnitude in permeability to sulforhodamine and bovine serum albumin (BSA), respectively [30].

Thermal ablation is a more economically favorable and safe method compared to the other diffusion enhancement techniques, while significantly improving drug diffusion and the breadth of drugs that may be used for TDD. It has been observed that properly combining more than one enhancement technique may generate a synergistic effect, pending the treatment or therapeutic characteristics. Combining electroporation with sonophoresis results in two different types of disruptions to the SC structure simultaneously, while electroporation also adds to electroporetic diffusion of the drug.

When electroporation is combined with iontophoresis, the electroporation increases SC permeability while iontophoresis adds a convective diffusion force to the diffusing particles. A similar effect occurs when iontophoresis is combined with microneedle treatments that provide direct access to the vascularized skin layers [22].

2.5 Impact of Heat on Diffusion

As was discussed in Section 2.3, equation (2.3) for particle diffusivity in a Stokesian system experiences its temperature impact primarily from the viscosity term that exponentially decreases with increasing temperature. This reduction in viscosity is primarily attributed to increased particle energy and reduced molecular organization due to the addition of heat to the system. As such, the Stokesian system's activation energy is determined based on the activation energy for the viscosity of the medium, which is determined by the increase in free volume due to expansion with increasing temperature [25].

In a Non-Stokesian system, the increase in diffusivity with respect to temperature is two-fold, resulting from: the increase in free volume and the increase in the overall rate of formation of holes. This is expressed in equation (2.5), for the probability function based diffusivity, in the exponential factor of the viscosity in the Stokesian diffusivity term and in the exponential Arrhenius term. Furthermore, activation energy in diffusion through a polymer matrix is greater than in diffusion through a liquid. Therefore, the temperature contribution to the diffusivity for a Non-Stokesian system is of greater value. As can be seen in Table 2.2, the type of polymer through which the particle is diffusing greatly impacts the activation energy of the diffusing particle. As natural rubber is not galvanized, the polymer strands slide past each other when undergoing tensile stress and allow for more

open diffusion paths. On the other hand, polyisobutylene is a crosslinked butyl rubber that makes it very resilient. This type of infrastructure contains more restricted diffusion paths, similar to the brick-and-mortar structure exhibited in the SC [25].

Table 2.2 Activation Energy for Diffusion within Polymers

Diffusant	E_{act} (kJ mol^{-1})	
	Natural rubber	Polyisobutylene
Hydrogen	25	32
Oxygen	31	45
Nitrogen	36	49
Carbon dioxide	37	49
Methane	36	—
Ethane	38	—
Propane	38	—
n-Butane	45	70
Isobutane	46	73
n-Pentane	52	67
Isopentane	47	76
Neopentane	51	75

Stein, Wilfred D., and W. R. Lieb. *Transport and Diffusion across Cell Membranes*. Orlando: Academic, 1986, 94-102.

2.6 Impact of Heat on Skin Permeability

In TDD, the drug crosses two diffusion membranes: the polymer matrix in the patch and the SC with two different fluxes that are related to each other by the partition coefficient of the aqueous solution of the drug in the reservoir with respect to the SC. Once the drug partitions from the reservoir to the SC, it also partitions into the deeper levels of the skin that can be termed aqueous, as well (Figure 2.7).

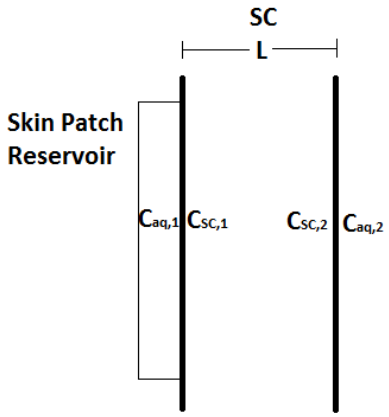

Figure 2.7 Simplified model of diffusion starting from the patch reservoir, across the polymer matrix and SC*.
* The dimensions of the SC are exaggerated compared to the skin patch reservoir.

$$K_m = \frac{C_{SC,1}}{C_{aq,1}} = \frac{C_{SC,2}}{C_{aq,2}} \tag{2.6}$$

$$J_{SC} = PA\left(C_{aq,1} - C_{aq,2}\right)$$

$$= \frac{D_{SC}}{L} A(C_{SC,1} - C_{SC,2})$$

$$= \frac{K_m D_{SC}}{L} A(C_{aq,1} - C_{aq,2}) \tag{2.7}$$

$$P = \frac{K_m D_{SC}}{L} \tag{2.8}$$

The flux of the drug diffusing from the reservoir to the deeper skin levels is related to the product of the SC permeability (P) and the area (A) through which the drug is diffusing (first part of equation (2.7)). As with previous flux calculations, this one is proportional to negative concentration gradient ($C_{aq,1}$ and $C_{aq,2}$). The second form of the flux equation substitutes the SC permeability for the ratio of the SC diffusivity (D_{SC}) and the diffusion path length (L). As can be seen from equation (2.6) for the partition coefficient

of the SC, K_m, the concentrations on the surface of the membranes on the aqueous sides are related to the concentrations on the SC side of the membranes ($C_{SC,1}$ and $C_{SC,2}$). This relationship is equivalent to the ratio of the solubility of the diffusant in the SC medium with respect to the aqueous medium at each of the separating barriers. Therefore, by substituting the SC partition coefficient relationship into the second part of equation (2.7), the final form of the flux equation with respect to the concentrations in the aqueous regions is obtained. This form of the flux equation holds the advantage of requiring the aqueous concentrations, which are easily obtained compared to the concentrations in the SC [25].

From equation (2.8), it is evident that any modifications to the SC permeability are related to the diffusivity across the SC. Permeability is a rate phenomenon that contains contributions from partitioning and intermembrane diffusion. The diffusivity through the SC follows Non-Stokesian behavior, as the SC is not fluid. Diffusion through the SC is similar in concept to diffusion through a polymer matrix, but its permeability varies between individuals based on genetics, temperature, lifestyle and body part. Therefore, temperature impacts SC permeability both from the Stokesian diffusion diffusivity term and the exponential Arrhenius term. An increase in temperature results in an increase in SC permeability and drug solubility because there is an increase in free volume and its formation. This is also expressed in the lipid fluidization or melting around the corneocytes, which permits increased movement in the lipid medium [31].

2.7 Case Studies – Supporting Research

At this point, computational diffusion studies of TDD are quite scarce. Most research and testing on skin patches relies on clinical trials including those for dosage determination, which poses high risk to the test subjects. The TDD clinical trial reports primarily rely on questionnaire data collected from the subject and their respective blood tests. This poses several issues in obtaining an exact analysis of any skin patch that is released into the market, as skin permeability and individual sensitivity to drug uptake varies between individuals. As skin permeability is quite variable and side effects are possible, clinical trials cannot be completely eliminated but they can be designed in a safer manner by computational estimation of the drug's diffusivity. Three case studies will be discussed. The first Nicotine patch analysis is qualitatively based on clinical trials, whereas the second research will discuss the computational determination of the diffusivity of nicotine diffusing through the skin patch copolymer matrix. Finally, the clinical trial report for the SYNERA Heated Lidocaine Tetracaine patch will be discussed, as it is the patch being tested in this study.

2.7.1 Nicotine Patch

As mentioned above, most pharmacokinetic analyses of TDD patches are rarely quantitative. One such analysis was used to compare the diffusion profile of the 21-mg/24-hour NiQuitin Patch (Nicoderm CQ in the USA and Nicabate in Australia) with that of the Nicorette Invisi 25-mg/16-hour patch. The test subject pool consisted of fifty smokers that smoke 11-40 cigarettes daily, twenty one female and twenty nine males. The NiQuitin patch is applied for twenty four hours, with an initial dose of 21 mg. The Nicorette Invisi patch is prescribed for sixteen hours of application, with a starting dose of 25 mg. The

subjects received both forms of treatment consecutively, with half of the subjects starting with the NiQuitin treatment followed by the Nicorette treatment while the other twenty five subjects went through the treatments in the reverse order. The control was the NiQuitin patch worn for sixteen hours rather than the prescribed twenty four hours. The pharmacokinetic profile for the TDD treatments was obtained from blood samples drawn from the patients up to thirty two hours post-initiation of treatment. All patient incidents were reported via a questionnaire [32].

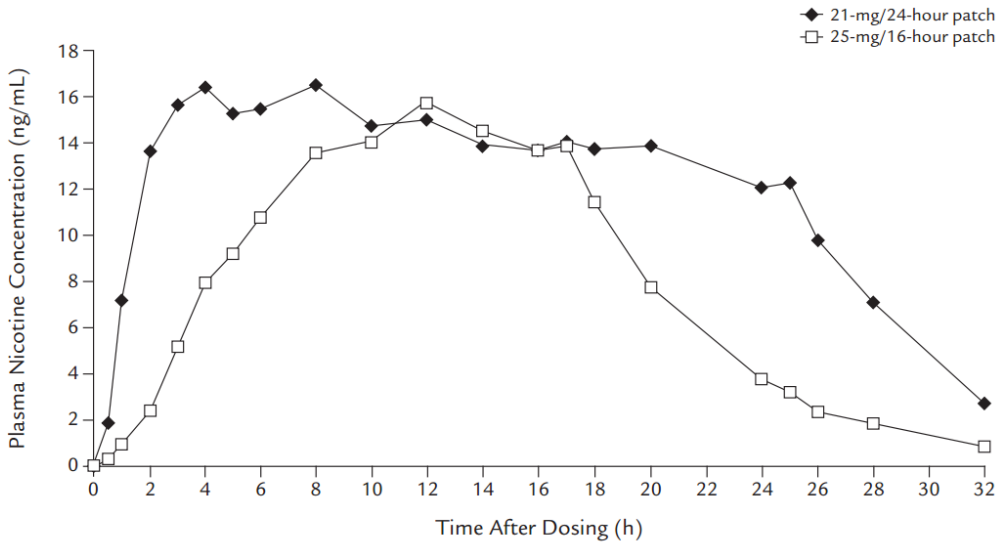

Figure 2.8 Mean plasma nicotine concentrations during exposure to the NiQuitin and Nicorette Invisi transdermal Nicotine systems.
Deveaugh-Geiss, Angela M., L. H. Chen, M. L. Kotler, L. R. Ramsay and M. J. Durcan. "Pharmacokinetic Comparison of Two Nicotine Transdermal Systems, a 21-mg/24-hour Patch and a 25-mg/16-hour Patch: A Randomized, Open-label, Single-dose, Two-way Crossover Study in Adult Smokers." *Clinical Therapeutics* 32.6 (2010): 1140-148.

The results indicated that the NiQuitin Patch provided the larger overall nicotine exposure, as indicated by its larger area under the curve (AUC) in Figure 2.8. Also, the maximum plasma nicotine concentration was higher for the NiQuitin patch and was reached faster than for the Nicorette patch, which exhibited a more gradual nicotine release profile without the initial concentration spike seen for the NiQuitin patch. Most patients

reported adverse events for both treatments. The adverse events were classified as primarily mild, as they were attributed to irritation due to the patch itself and some dizziness, with one subject requiring cessation of treatment. It was not mentioned which of the treatments led to the latter case nor did the article indicate if it was the patient's first or second round of TDD treatment. Individual variation in response to medication exemplifies the need to computationally analyze TDD treatments prior to clinical trials. Furthermore, the diffusivity differences between both patches were neither extensively analyzed nor were they calculated for the initial increase in nicotine plasma concentration for both patches. Computational analysis of the diffusivity through the polymer matrix for both patches could put into perspective the significance of their individual design parameters and their implications [32].

2.7.2 Computational Determination of Diffusivity

The article *New Screening Methodology for Selection of Polymeric Matrices for Transdermal Drug Delivery Devices* [1] is the only research directed at the computational analysis of a drug diffusing through a polymer matrix in the skin patch. In this case, the nicotine patch was used to validate the results. The methodology in this research is the basis for the research discussed in this thesis, except that the skin patch analyzed is the SYNERA local anesthetic heated lidocaine-tetracaine patch. As this skin patch contains a diffusion enhancing component and there are two diffusing molecules, some adjustments will be made to the modified Duda-Zalinsky equation (DZE) constructed by Falcone in his computational analysis of the diffusivity of nicotine [1].

Diffusion through the TDD patch can be modeled as diffusion through a planar surface. Crank provided the following solution for the concentration profile in planar diffusion:

$$C = \frac{M}{2\sqrt{\pi D t}} e^{-x^2/4Dt} \tag{2.7}$$

$$\frac{M_t}{M_\infty} = \frac{4}{l}\left[\frac{D}{\pi}\right]^{-2t^2} \quad \text{When } \frac{M_t}{M_\infty} \leq 0.5 \tag{2.8}$$

In equation (2.7), C is the solute concentration, D is the diffusivity, t is the time, x is the diffusion length. The relationship in equation (2.8) for the ratio of the solute concentration (M_t) at time t with respect to the initial concentration M_∞ holds true for the following boundary condition: concentration at time t is equal to or less than half the initial concentration [1].

For the purpose of analysis of a drug diffusing through a polymer matrix, the diffusion process must be modeled by the free volume theory. This model describes diffusion as a mechanical model that involves concurrent exchange between the free and occupied volumes. Therefore, the specific gap free volume in equation 2.5 is calculated based on the ratio of the molar gap free volume ($\hat{V}_{FH}$) with respect to the molecular contribution of each of the constituents (the ratio of the individual weight fractions, w_i, with respect to their molecular weights, M_i, polymer and drug) to the system:

$$\bar{V}_{FH} = \frac{\hat{V}_{FH}}{\frac{moles\ of\ diffusing\ units}{g}} = \frac{\hat{V}_{FH}}{\frac{w_1}{M_1} + \frac{w_2}{M_2}} \tag{2.9}$$

Equation (2.9) was incorporated into Vrenta and Duda's equation (equation (2.5)) to form equation (2.10). Since in the nicotine patch, nicotine diffuses through a block copolymer matrix, the second weight fraction in the denominator of equation (2.9) is multiplied by the ratio of the weight fraction of each of the polymers in the matrix divided by their molecular weight. Furthermore, the effect of the copolymer matrix was carried over to the calculation of the solvent critical molar volume jumping unit with respect to the polymer jumping unit that is designated as ε (eq. (2.11)) [1].

$$D_1 = D_0 e^{(-E/kT)} e^{\left\{-\frac{\gamma[W_1\bar{V}_1 + W_2(W_{2a}\varepsilon_{12a}\bar{V}_{2a} + W_{2b}\varepsilon_{12b}\bar{V}_{2b})]}{\bar{V}_{FH}}\right\}} \tag{2.10}$$

$$\varepsilon_{12a} = \frac{M_{1j}\bar{V}_1}{M_{2ja}\bar{V}_{2a}} \qquad \varepsilon_{12b} = \frac{M_{1j}\bar{V}_1}{M_{2jb}\bar{V}_{2b}} \tag{2.11}$$

$$\frac{4}{3}\pi R_0^3 = \frac{m}{\rho}$$

$$\frac{4}{3}\pi R_0^3 = \frac{M_W}{\rho N_A}$$

$$R_0 = \left[\frac{3M_W}{4\pi N_A \rho}\right]^{1/3} \tag{2.12}$$

One of the advantages of this methodology lies in the usage of the hydrodynamic radius of the drug, as the critical volume for diffusion relies on the resulting effective volume due to the rotation of the molecule about its center of gravity. The molecule's effective center of rotation does not necessarily lie at the center of the molecule and can be impacted by secondary interactions of the molecule's functional groups. The

hydrodynamic radius (R_0) is obtained by relating the spherical molar volume of the drug and its density, which should give an over estimation of the actual molar volume of the drug as it is representative of the radius that stems from the rotation of the molecules (equation (2.12)). Energy values were obtained through the Tonge and Gilbert equation.

Diffusivity values, obtained for nicotine, based on these computation were compared to diffusivity values obtained from the concentration profile of the investigated nicotine patch. The concentration profile for the nicotine patch was generated from UV spectrophotometry absorption readings of samples extracted periodically from a Franz-Cell apparatus, which had the nicotine patch clamped to its cell top opening thereby permitting nicotine diffusion (Figure 2.9) [1].

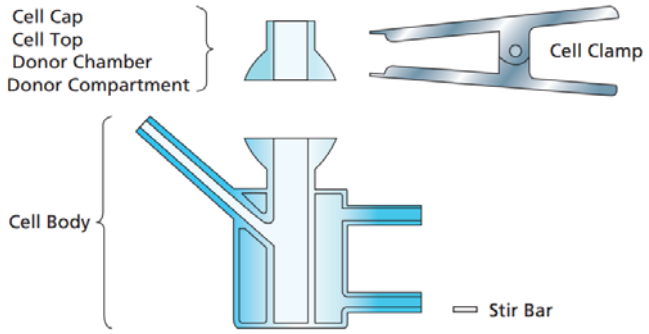

Figure 2.9 Components of PermGear's Franz Cell Apparatus.
PermeGear. http://www.permegear.com/franzatfaqs.htm

As can be seen in the results in Figure 2.10, below the calculations for the cumulative amount released, the product of the diffusivity and the time point in the diffusion process, for both experimental and calculated values are close with the percent error increasing with respect to the diffusion time. The final diffusivity results, summarized in Table 2.3, show that the calculated diffusivity is of the same order of magnitude as the experimental diffusivity, with an over estimation of approximately 17%. To emphasize the significance of this result, the diffusivity values obtained were compared to the diffusivity

values for nicotine provided in the literature, which stated that the diffusivity range is between 10^{-9}-10^{-10} cm^2/s. Therefore, this computational model is fitting to describe diffusion through polymer matrices in TDD patch systems [1].

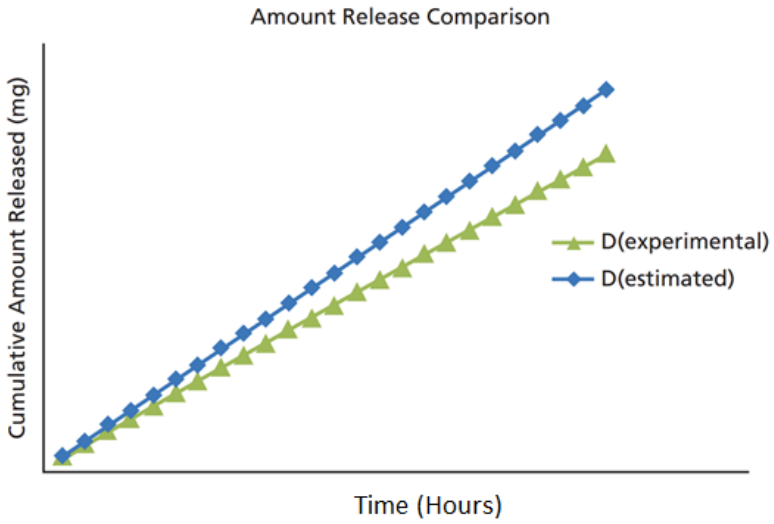

Figure 2.10 Cumulative release comparison for the experimental and estimated nicotine diffusivity values.
Falcone, R., Jaffe, M. and Ravindra, N.M., New screening methodology for selection of polymeric matrices for transdermal drug delivery devices, Bioinspired, Biomimetic and Nanobiomaterials, Volume 2 Issue BBN2, p. 65-75, 2013.

Table 2.3 Comparison between experimental and calculated nicotine diffusivity values

Property	Value (cm^2/s)
D (experimental)	$1{\cdot}467 \times 10^{-9}$
D (calculated)	$1{\cdot}781 \times 10^{-9}$

Falcone, R., Jaffe, M. and Ravindra, N.M., New screening methodology for selection of polymeric matrices for transdermal drug delivery devices, Bioinspired, Biomimetic and Nanobiomaterials, Volume 2 Issue BBN2, p. 65-75, 2013.

The method of computation of diffusivity, used for nicotine, is the basis for the procedure used in the research discussed in this thesis. In this research, Galen

Pharmaceitical's Heated Lidocaine/Tetracaine local anesthetic patch is analyzed, with added corrections to the diffusivity equation proposed by Falcone so as to account for the impact of the diffusion enhancement on the diffusivity of the solutes.

2.7.3 SYNERA Heated Lidocaine-Tetracaine Patch

Lidocaine has been used for topical anesthesia since the 1980's in various forms. It has evolved over several cycles from a cream to a TDD patch where the lidocaine active is held as part of a eutectic mixture. Some of the hallmarks of the development of this local anesthetic include the following forms: cream in the form of a submicron emulsion (SME), lidocaine/prilocaine eutectic mixture in regular cream, lidocaine/tetracaine eutectic mixture in regular cream, lidocaine/tetrcaine eutectic mixture in SME cream, lidocaine/epinephrine patch (Iontocaine,1995), lidocaine patch (Lidoderm, 1999), lidocaine/ultrasound patch (SonoPrep, 2004) and finally, lidocaine/tetracaine heated patch (Synera, 2005 – the gold standard).

Eutectic mixtures are normally mixtures of two components that together develop different physicochemical properties compared to their separate pure forms, which is due to moderate molecular interactions between the individual constituents. These properties do not impact the individual constituents' inherent molecular orientation, rather some of their characteristics are modified. As an example, the eutectic mixture's melting point is significantly lower than either constituent's individual melting point, which poses the advantage of lowering the processing temperature of either of the constituents if called for.

In the case of the lidocaine/prilocaine eutectic mixture, the melting point of the system is 32°C while lidocaine's melting point in its pure form is 68°C. As this melting point is slightly below skin surface temperature, the lidocaine anesthetic assumes a molten

form upon contact with the skin. The eutectic mixture's physical properties facilitate more rapid skin penetration of lidocaine with respect to its pure form. Therefore, eutectic mixtures have been found to enhance transmembrane diffusion.

In the past, the lidocaine anesthetic cream has been formulated as a eutectic mixture with prilocaine; but studies have shown to exhibit competitive diffusion properties. Lidocaine's diffusion is more influenced by the partition process, whereas prilocaine's diffusion is more influenced by the transport process. A diffusion study of the lidocaine/prilocaine eutectic mixture showed that maximum skin permeation occurs for mixture compositions where the solid and liquid phase are not at equilibrium. This is indicative of questionable stability of the eutectic mixture formulation.

The latter observation was corroborated by a thermal analysis that compared the stability of the lidocaine/prilocaine eutectic mixture with the stability of the lidocaine/tetracaine eutectic mixture. The authors found that the lidocaine/tetracaine eutectic mixture's crystallization peaks, observed through modulated temperature differential scanning calorimetry (MTDSC), are in close temperature proximity to the lidocaine/prilocaine eutectic mixture's crystallization peaks. This implies that the lidocaine/tetracaine eutectic mixture contains more intermolecular interacting groups, thereby preventing crystallization out of formulation of either constituent in the binary mixture. It is evident from the molecular structures of lidocaine and tetracaine (Figure 2.11) that both molecules have the same functional groups with some structural differences and comparable molecular weights, which explains their similar physical properties.

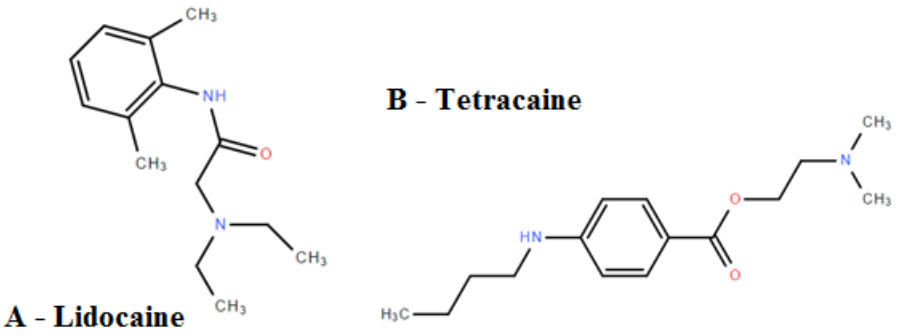

Figure 2.11 Molecular structures of lidocaine and tetracaine labeled A and B, respectively.

The Synera heated patch (Figure 2.12) was compared in a clinical trial setting to the lidocaine/prilocaine cream (EMLA). The Synera patch contains a eutectic mixture of 70 mg of lidocaine and 70 mg of tetracaine, with a suggested application time of at least twenty minutes – preferably thirty minutes, prior to local procedure. The lidocaine prilocaine cream provides with a 25 mg/mL dosage and should be applied one hour prior to local procedure. The Synera patch contains an iron nanoparticle and carbon heating pod on the top layer of the patch that is covered by a perforated covering, which exposes the heating pod to oxygen upon opening of the packaging and induces an exothermic oxidation of the iron nanoparticles that locally raises the skin surface temperature by 5°C. As previously discussed, the added heating component provides additional energy to the diffusing particles as well as promotes fluidization of the lipid matrix in the SC that could explain the shorter anesthetic application time.

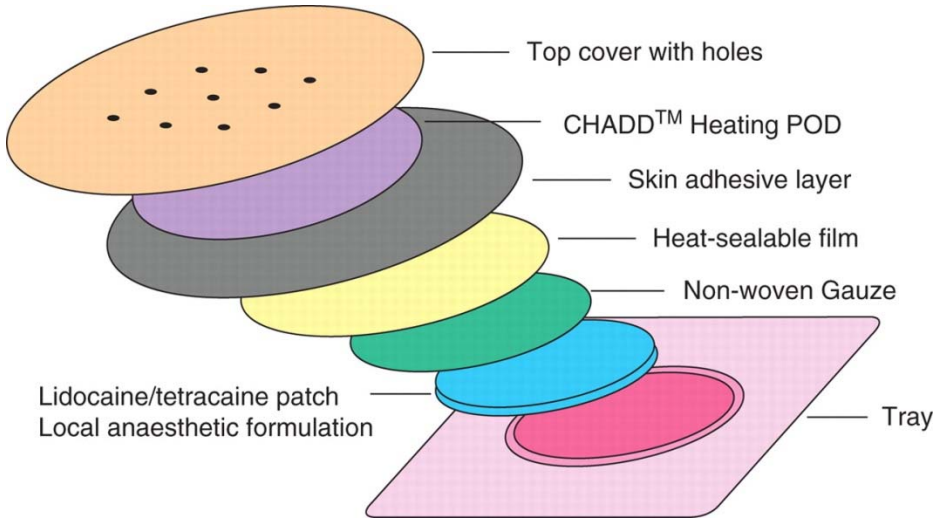

Figure 2.12 Layer by layer breakdown of the Synera heated lidocaine/tetracaine heated patch.
Sawyer, J., S. Febbraro, S. Masud, M. A. Ashburn, and J. C. Campbell. "Heated Lidocaine/tetracaine Patch (SyneraTM, RapydanTM) Compared with Lidocaine/prilocaine Cream (EMLA(R)) for Topical Anaesthesia before Vascular Access." *British Journal of Anaesthesia* 102.2 (2009): 210-15.

The investigation study group consisted of 82 healthy adults (37 males, 45 females) with varying skin types that received both anesthetic treatments simultaneously in two separate, but equivalent, skin locations. Both anesthetics were applied for 10, 20, 30 and 60 minutes prior to a vascular access procedure. Pain intensity was assessed by the subjects using a 100 mm visual analogue scale (VAS), with skin or any other side effects being visually inspected. The reported median VAS score was significantly lower for the Synera patch compared to the lidocaine/prilocaine cream for all time points leading up to thirty minutes; yet similar VAS scores were given to both anesthetics at the 60 minutes time point. Overall, it was deduced that the Synera lidocaine/tetracaine patch is more effective than the lidocaine/prilocaine cream due to it faster penetration. It is important to emphasize the significance of a computational model for this type of investigation, as opinion based pain evaluations are very individual because different people have different pain thresholds

and tolerances. Therefore, as this comparison validates the advantages of the Synera patch, it is of purely qualitative value.

Anesthetics have been shown to be of high skin penetration efficacy with skin fluidization properties. This is counterintuitive as anesthetics primarily perform their function by inhibiting protein-mediated transport processes that take part in the body's signaling process. Yet further investigation elucidated that, in addition to the anesthetic's inhibitory character, it also behaves similarly to a plasticizer in a polymer. Plasticizers are small molecules that disrupt intermolecular interactions in polymers, thus reducing polymer brittleness and increasing its ductility with respect to a certain temperature. In effect, this change in physical properties results from the reduction in the glass transition temperature of the polymer. Therefore, plasticizers serve to increase diffusion rates in polymers. Similarly, at high concentrations, anesthetics actually increase membrane permeability. Anasthetics fluidize lipid bilayers and biological membranes, which signifies that the Synera heated lidocaine/tetracaine patch has an additional inherent diffusion and permeability enhancer upon SC saturation. Despite anesthetic potency being an equilibrium phenomenon that relies on anesthetic partitioning, membrane permeability is also influenced by the actual intermembrane diffusion.

CHAPTER 3

EXPERIMENTAL APPROACH

3.1 Impact of Heat/Composition

Computational research in this area has focused on the standard skin patch, to utilize a modified version of the DZE to predict drug diffusion in a noninvasive manner prior to testing of patches. It is of great importance to validate these modifications for other formulations of patches with varying matrices, drug actives and especially diffusion and permeability enhancers. Diffusion and permeability enhancements are of significant value for future formulations, as they will not only improve the diffusion efficiency of the drug, but will also provide an opportunity for the utilization of TDD to a wider range of therapeutics. As discussed extensively in the previous chapter, the heat enhancement in the Synera patch adds energy for partitioning of both lidocaine and tetracaine and it helps to fluidize the SC by liquefying the lipid components in the polymer matrix and facilitating less resistive diffusion paths. Furthermore, the Synera patch involves a eutectic mixture as its active component as opposed to a single drug active.

The free hole volume is a function of the structure of the polymer matrix and diffusant occupying volume in relation to the reference temperature relative to the glass transition temperature. Equation (3.1) shows Fierro *et al.*'s method of computing the free volume.

$$\hat{V}_{FH} = w_1 K_{11}\left(K_{21} - T_{g1} + T\right) + w_2 K_{12}(K_{22} - T_{g2} + T) \tag{3.1}$$

K_{11} and K_{21} are free volume parameters for the active components, which can be retrieved via nonlinear regression of the equation for the base ten logarithm of the difference in viscosity between the glass transition and reference temperatures [35]. K_{12} and K_{22} are the free volume parameters for the polymer matrix. T is the reference temperature and w_i and T_{gi} are the weight fractions and glass transition temperatures of component "i", where the subscript 1 denotes the drug active and 2 denotes the polymer matrix. It is important to note in this equation that only one active at a time is included in this calculation. This is acceptable because the diffusion of drug actives is not codependent [1].

K_{11}, K_{21} and K_{12}, K_{22} are related to the Williams-Landel-Ferry (WLF) constants, C_1, C_2. K_{12} is related to the critical molar volume and the overlap factor. In combination with a nonlinear regression with respect to the Doolittle equation for viscosity, K_{12}, can be used to solve for the overlap factor. The WLF constants for the polymer were retrieved from linear regression of values found in the literature for varying PVA concentrations [36]. The glass transition temperature for lidocaine and tetracaine was calculated by a group contribution method (equation (3.2)). This method computes the product of the molecular weight and "glass transition temperature" contributed by individual parts of the polymer backbone (denoted "i") and side chains (denoted "j"), distributed over the entire molecular weight [37].

$$T_g = \frac{1}{M}\left[\sum_i (T_g M)_i + \sum_j (T_g M)_j\right] \tag{3.2}$$

3.1.1 Modifications to DZE

The energy and viscosity components of the diffusivity calculations performed in this research are in agreement with those performed in the computational analysis of nicotine discussed in Section 2.7.2, with a few modifications. In this case, the solute is a binary system and the matrix is being treated as one polymer component. Furthermore, the temperature analysis will consider the additional 5°C added by the Synera skin patch heating component.

3.1.2 Composition Calculations

The composition of the drug actives was taken as 1:1 as listed in the specifications of the drug. Based on the list of ingredients of the patch, the primary polymer contribution to the diffusion membrane was attributed to polyvinyl alcohol. TGA was used to assess the weight contribution of the polymer matrix to the TDD patch system. Due to the proprietary nature and confidentiality of this patch, these results and analyses will not be discussed in this thesis.

3.1.3 Energy Calculations

The energy calculation was computed based on the Tonge and Gilbert computation, equation (3.1) [33]. To obtain the partitioning energy (E^*) involved in either of the drugs' diffusion through the polymer matrix, the cohesive energy density (δ) of lidocaine tetracaine was computed based on equation (3.2). The cohesive energy density is also representative of the constituent's solubility. The enthalpy of vaporization (H), subtracted by the product of the ideal gas constant (R) and the temperature in kelvin (T), represents

the cohesive energy of the molecule that is stored in its own molecular volume unit (V_M). The cohesive energy density for PVA was obtained from the literature. Equation (3.3) shows the Yamada and Gunn equation [34] for the molecular volume at the testing temperature, as the cohesive energy of the molecule varies with temperature. All properties denoted with the subscript "c" represent the critical properties of the molecule, at which point condensation of vapor does not occur despite temperature elevation.

$$log_{10}(E^*) = 0.8988 \ln\left(\log\left[(\delta_1 - \delta_2)^2 \hat{V}_s\right]\right) + 2.8377 \tag{3.1}$$

$$\delta_{L,T} = \sqrt{\frac{H - RT}{V_M}} \tag{3.2}$$

$$\hat{V}_s = V_c(0.29056 - 0.08775\omega)^{(1-\frac{T}{T_c})^{2/7}} \tag{3.3}$$

$$\omega = -log_{10}(p_r^{sat}) - 1, at\ T_r = 0.7 \tag{3.4}$$

$$T_r = \frac{T}{T_c}; p_r^{sat} = \frac{p^{sat}}{p_c}$$

$$\ln\frac{p^{sat}}{p^0} = -\frac{\Delta H_{vap}}{ZR}\left[\frac{1}{T^{sat}} - \frac{1}{T^0}\right] \tag{3.5}$$

$$Z = 1 + \frac{9PT_c}{128P_cT}\left[1 - 6\left(\frac{T_c}{T}\right)^2\right] \tag{3.6}$$

The saturated liquid molar volume requires the calculation of the acentric factor (equation (3.4)), a measure of corresponding state for saturated hydrocarbons [38]. All the properties denoted with the letter "r" refer to the reduced value of that property. This equation is only valid for the reduced saturated vapor pressure (p_r^{sat}) at a reduced temperature value of 0.7. The Clausius Clapeyron equation (equation (3.5)) for real gases

was used to calculate the saturated vapor pressure. This calculation was based on the pressure and temperature data at room temperature from the literature. The ideal gas Clausius Clapeyron equation has an added correction factor, Z, called the compressibility factor. The compressibility factor was estimated with the Berthelot equation (equation (3.6)).

3.2 Materials

Experimental process:

1. PermGear Franz-Cell apparatus (6-cell apparatus).

Table 3.1 Cell Dimensions (by cell number, from right to left)

Cell no.	Volume (mL)	Top Inner Diameter (cm)
1	11	1.5
2	10.6	1.5875
3	11.6	1.524
4	12.6	1.60

2. Hot water bath.
3. Water pump.
4. Synera skin patches.
5. Saline solution.
6. UV spectrophotometer.
7. 500 mg/L lidocaine in water stock solution.
8. 100 mg/L tetracaine in water stock solution.

9. Thermocouple.
10. IR camera.

For the experiments, a Franz cell apparatus was employed with a water pump for temperature control of the system. Saline served as the diffusion media in the cell body. As the patches were quite large, the clamp on its own was enough to keep the patch in place. Sample analysis was conducted via a UV spectrophotometer. Stock solutions prepared for the calibration curve were made of dilutions of 500mg/L lidocaine in de-ionized water and 100mh/L tetracaine in de-ionized water solutions.

3.3 Franz-Cell Apparatus

The Franz-Cell was connected to a hot water pump to maintain the temperature of the system. The water flows between the outer walls of the cell, while the inner cell contains a small magnetic stirrer set underneath a coil to induce constant mixing when the apparatus is turned on. The Synera patch was clamped without a cap, as its dimensions permit this construct. The cell bodies should be filled completely with saline and must form a meniscus in the cell top, so as to ensure constant surface contact of the patch diffusion site and the aqueous solution. Periodic samples of approximately 1 mL were taken at four different time points through a long needle that extends into the cell body via an inlet opening. To prevent disruption of the diffusion system, an equivalent volume of saline was added into the cell body after each sample extraction.

A calibration curve was set up from serial dilutions of the lidocaine and tetracaine stock solutions. 0.1 M hydrochloric acid was added to the stock solutions along with pH buffer no. 6, so as to promote solute dissolution. Based on literature values, the peak UV

absorbance wavelengths are 262±1nm [39] and 310±1nm [40] for lidocaine and tetracaine, respectively. As Beer's law states, for small absorbance values (between 0.01-1), the absorbance is linearly related to the sample concentration, diffusion length and extinction coefficient of the sample. Therefore, the linear regression equation obtained from the calibration curve for the stock solution and its dilutions provides a direct relationship to the active concentration in the sample. The diffusion profile for the drug is made up of a plot of the generated concentrations with respect to their sampling time. The concentration profile for a skin patch is linear until the concentration plateaus. The slope of the line prior to the leveling of the concentration is the diffusivity. For this wavelength range, quartz cuvettes must be used to obtain accurate readings. Table 3.2 lists the dilutions of the stock solutions, where C_0 is a concentration of 100 mg/L.

Table 3.2 Serial Dilution Concentrations for Lidocaine and Tetracaine's Calibration

Lidocaine Concentration		**Tetracaine Concentration**	
5 C_0	500mg/L	C_0	100 mg/L
3.25 C_0	325 mg/L	0.9 C_0	90 mg/L
2.5 C_0	250 mg/L	0.75 C_0	75 mg/L
1.75 C_0	175 mg/L	0.5 C_0	50 mg/L
C_0	100 mg/L	0.25 C_0	25 mg/L
0.75 C_0	75 mg/L	0.10 C_0	10 mg/L
0.5 C_0	50 mg/L		
0.25 C_0	25 mg/L		
0.10 C_0	10 mg/L		

3.4 Temperature Corroboration

Temperature corroboration in this experiment is important because it provides information on the functionality of the patch and the temperature stability of the diffusion system, whose temperature is maintained by the pumping of the water from the hot water bath. Thermocouples were placed between the cell body and its holder so as to record the temperature of the system. An IR camera is used to verify that the 5°C temperature increase reported by the manufacturer is accurate and persistent throughout drug administration. Based on the difference in the colometric temperature in the area of the patch compared to the temperature further down in the cell body, the induced temperature increase can be validated. As the SC is less than 3 μm in thickness, the temperature penetration depth is not of significance.

CHAPTER 4

RESULTS AND DISCUSSION

4.1 Computational Results

Table 4.1 shows the calculated hydrodynamic radius, the glass transition temperature and its corresponding viscosity for lidocaine and tetracaine. Table 4.2 is divided into three testing temperatures for lidocaine and tetracaine. As can be seen, tetracaine has a larger activation energy, due to its larger molecular weight. Initially, the impact of the heating pod was thought to have a large impact on the energy of the actives (Table 4.2). Based on the tabulated values with respect to temperature, the increase in additional available energy is not significant for such temperature differences.

Table 4.1 Calculated Hydrodynamic Radius, T_g and the Corresponding Viscosity for Lidicaine and Tetracaine

	Tg (K)	**μ (Pa-s)**	**R0**
Lidocaine	219.74	0.05594947	3.9588E-10
Tetracaine	268.105	0.013004086	3.9588E-10

The viscosity decreases with increasing temperature, but the results show that for all temperatures they are of the same order of magnitude. Therefore, their impact on the diffusivity is similar.

Table 4.2 Energy, Viscosity, Free Volume and Stokes Einstein Diffusivity Multiplier for Lidocaine and Tetracaine with Respect to Temperature Setting

	Property	Lidocaine	Tetracaine
T=303.15 K	E (J)	38678.63	43147.55
	μ (Pa-s)	0.003716002	0.00455435
	D0 (m/s^2)	1.50942E-06	1.03294E-06
T=308.15 K	E (J)	38713.12	43172.64
	μ (Pa-s)	0.003309274	0.003998203
	D0 (m/s^2)	1.7229E-06	1.19602E-06
T=310.15 K	E (J)	38726.97	43182.705
	μ (Pa-s)	0.003162641	0.003799714
	D0 (m/s^2)	1.81448E-06	1.26667E-06

Table 4.3 summarizes the WLF factors that are used to calculate the free volume parameters for the free volume. Lidocaine and tetracaine have similar critical molar volumes, which are less than a third of PVA's critical volume. Therefore, it may be deduced that the primary contribution to the overlap factor and the primary occupier of the free volume is PVA. The diffusivity values obtained with the DZE will not be extensively discussed for this system, as they were off by about two orders of magnitude with respect to the experimental diffusivities. This is attributed to the free volume calculations that need further fine tuning.

Table 4.3 WLF Constants and Critical Molar Volumes of PVA, Lidocaine and Tetracaine

	C1	C2	V* (cm^3)
PVA	17.4	51.6	313.8
Lidocaine	1.22534	3.69403	89.79595
Tetracaine	1.7934	4.76435	94.26971

4.2 Experimental Results

In order to quantify the concentrations of the samples taken from the Franz Cell apparatus at different points in the diffusion process, a UV absorption calibration curve for different known concentrations of lidocaine was set up. Pure lidocaine and tetracaine exhibit peak absorbance values at wavelengths of 262±1 nm and 310±1 nm, respectively. In this particular UV spectrophotometer, the absorbance peaks were observed at 262.5 nm and 310.5 nm for lidocaine and tetracaine, respectively.

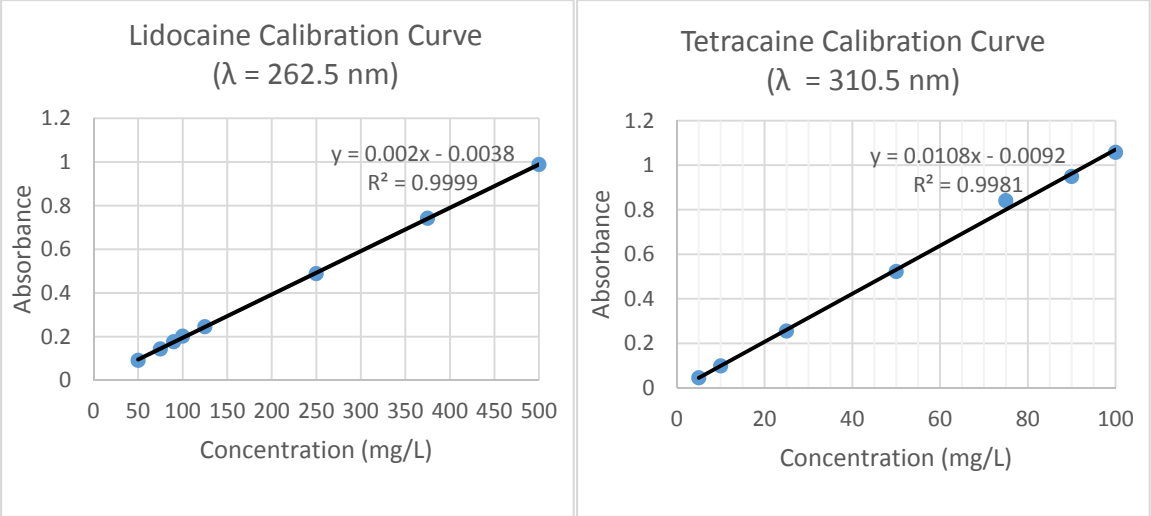

Figure 4.1 Lidocaine (left) and tetracaine (right) UV absorbance calibration curves.

According to the Beer-Lambert law, for absorption values between 0.01-1 (i.e. low concentrations), there is a linear relationship between the concentration and absorbance (equation (4.1)). The absorbance is related to the sample concentration (C) multiplied by the extinction coefficient of the sample (ε) and the path length of the light passing through (L), which is simply the width of the cuvette (10 mm in this case). This relationship held true for the solution concentrations plotted in Figure 4.1, that display an R^2 value for both linear regression lines close to one.

$$A = \varepsilon LC \tag{4.1}$$

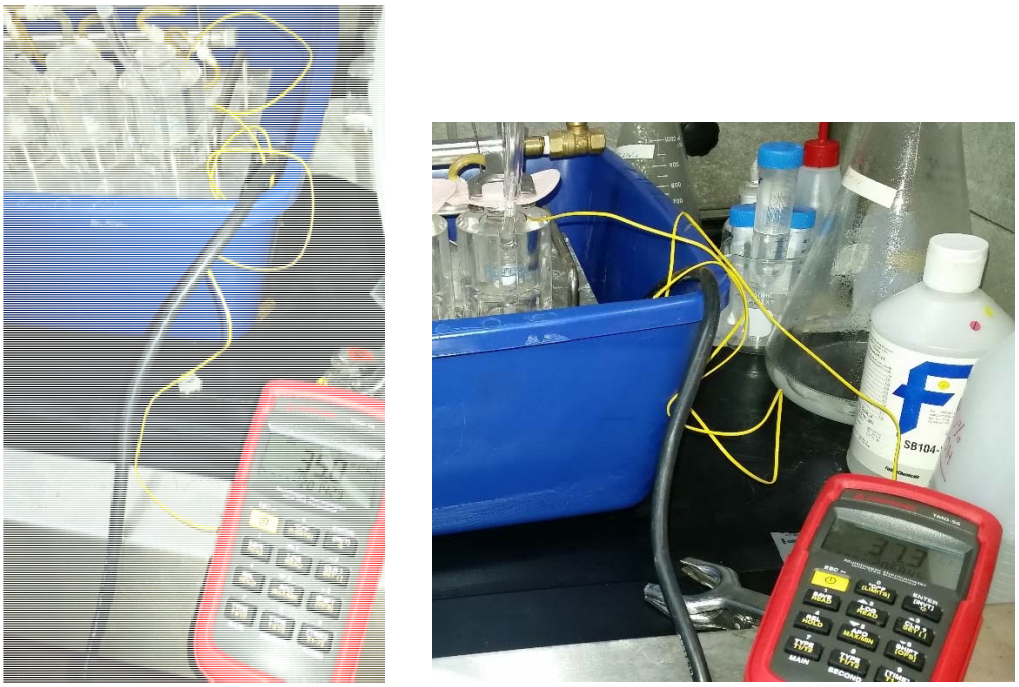

Figure 4.2 Franz Cell system temperature (°C) corroboration on the thermocouple.

As can be seen in Figure 4.2, the temperature was held stable throughout the diffusion process, with mild decrease in the last ten minutes. As will be discussed below, by the end of the first 5-10 minutes (temperature pending) the drug concentration peak is reached and maintained through the end of the run. The IR images (Figure 4.3, 4.4) confirm that the company statement that the heating pod provides a local increase in temperature of 5°C is correct.

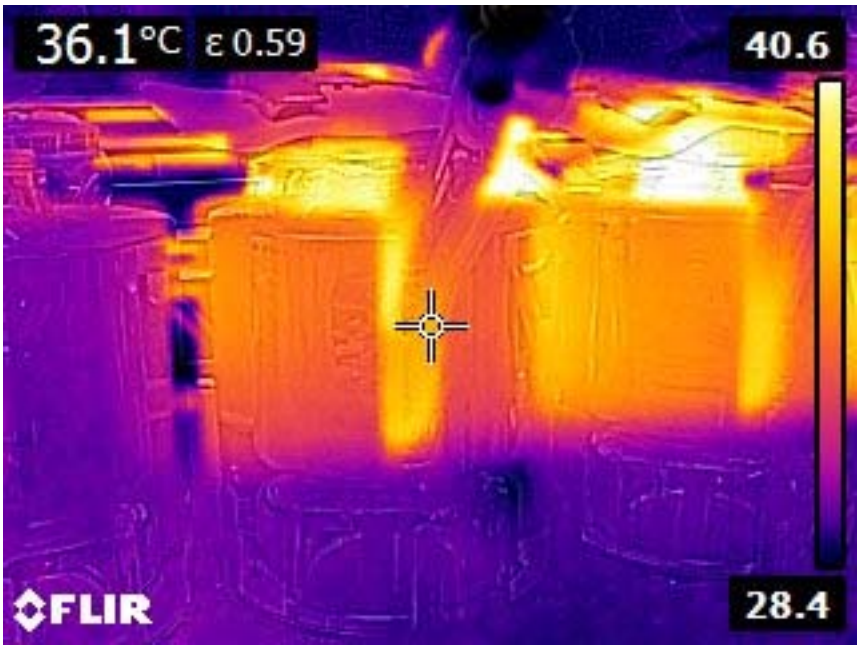

Figure 4.3 Thermal image of cells 3 and 4* during the diffusion run (side view).
* Cell 4 is the left cell and it is the nonheated control.

Figure 4.4 Thermal image of cells 1-4* during the diffusion run (top view).
* Cell 4 is the left cell and it is the nonheated control.

The side view (Figure 4.3) serves to show the heat diffusion distance, as there is a heat gradient throughout the length of the cell body where the maximum temperature is at

the top and the minimum is at the bottom. Despite this gradient it may be assumed that when the Synera patch is applied the local SC temperature matches the maximum temperature, which is the critical determinant of the drug penetration. Figure 4.4 confirms that the control did not experience the oxidation reaction as a result of obstructing the top openings with tape. The temperature difference was further confirmed by the color difference between the top view of the patch that was used as the control and the rest of the cells.

Figure 4.4 below contains the lidocaine diffusion profile at 30°C, 35°C and 37°C. The diffusion with respect to time at 30°C reaches its peak cumulative release at after 10 minutes, whereas this time period is shortened to 5 minutes for diffusion at 35°C and 37°C. At 30°C the control, the patch that did not undergo oxidation, exhibited a significantly reduced supplied dosage. Yet for the higher testing temperature, the peak concentration is similar with respect to the control. As can be seen in Figures 4.4A and 4.4B, the results collected for cell 3 peak at twice the lidocaine released, which compared to the rest of the cells. This is the reason that the tests results in Figure 4.4 C were only performed on the first two cells. The experiments in Figures 4.4A and 4.4B were performed on the same day and the discrepancy was correlated to a faster spin rate of the magnet in cell 4, which initially went unnoticed. A research conducted on the Franz Cell apparatus showed that stirring speed impacts the amount of time a dye gets dispersed in the Franz cell and the time it takes it to reach up the sampling arm. On the other hand, too high of a stirring speed may result in vortexing, which can disrupt the diffusion cell [41].

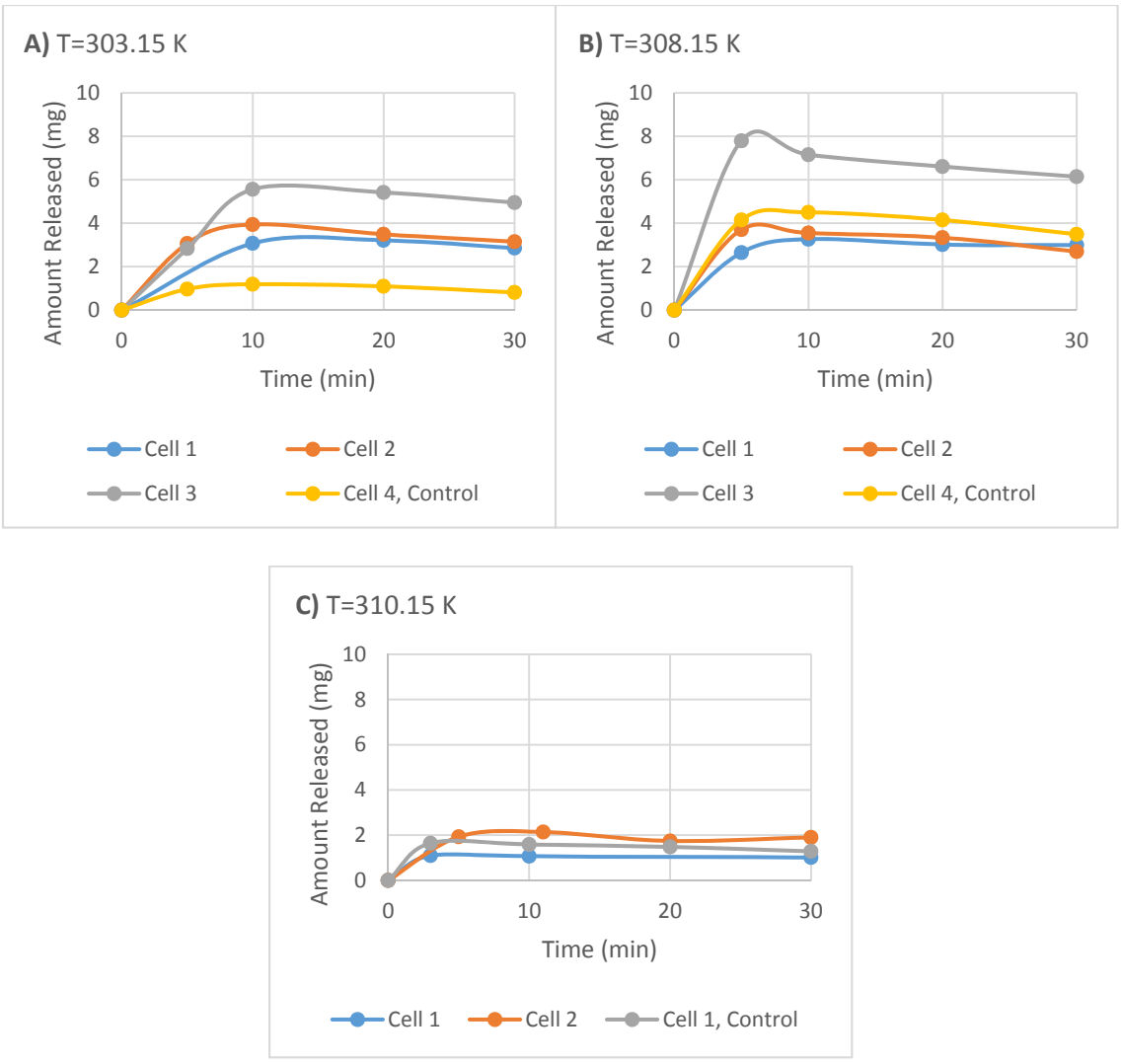

Figure 4.4 Cumulative accumulation of lidocaine with respect to time at A)30°C=303.15 K, B) 35°C=308.15 K and C) 37°C=310.15 K.

Figure 4.5 displays the mass of accumulated tetracaine in the cell body. A similar diffusion pattern to that of the lidocaine was observed, with peak accumulation occurring at the 10 minutes and 5 minutes time point for 30°C and 35-37°C, respectively. The same discrepancy with respect to cell 4 was observed in the tetracaine results, as well. It is important to note that despite the initial lidocaine and tetracaine dosages being identical in the patch regimen, approximately double the amount of lidocaine compared to tetracaine diffuses into the cell. This can be explained by lidocaine's lower octanol:water partition

ratio of 182 at pH 7.3 compared to tetracaine's higher partition ratio of 5370 at pH 7.3 [42]. As the cell media is saline, 0.9% NaCl aqueous solution in water, tetracaine's hydrophobic character results in a hindered diffusion of tetracaine. The Synera patch prescribing information discussed its clinical trials that revealed that approximately 1.7 mg and 1.6 mg of lidocaine and tetracaine, respectively, were absorbed by the subject [43]. The mass of lidocaine was substantially below the maximum dose released in the Franz cell, which can be explained by the skin barrier that is posed by the skin. In contrast, the reported peak accumulation for tetracaine was slightly higher than the experimental results in Figure 4.5 C. This may be attributed to tetracaine's higher partition ratio that compensates for its reduced diffusion into aqueous solution, by increasing its probability of diffusing through the hydrophobic SC barrier.

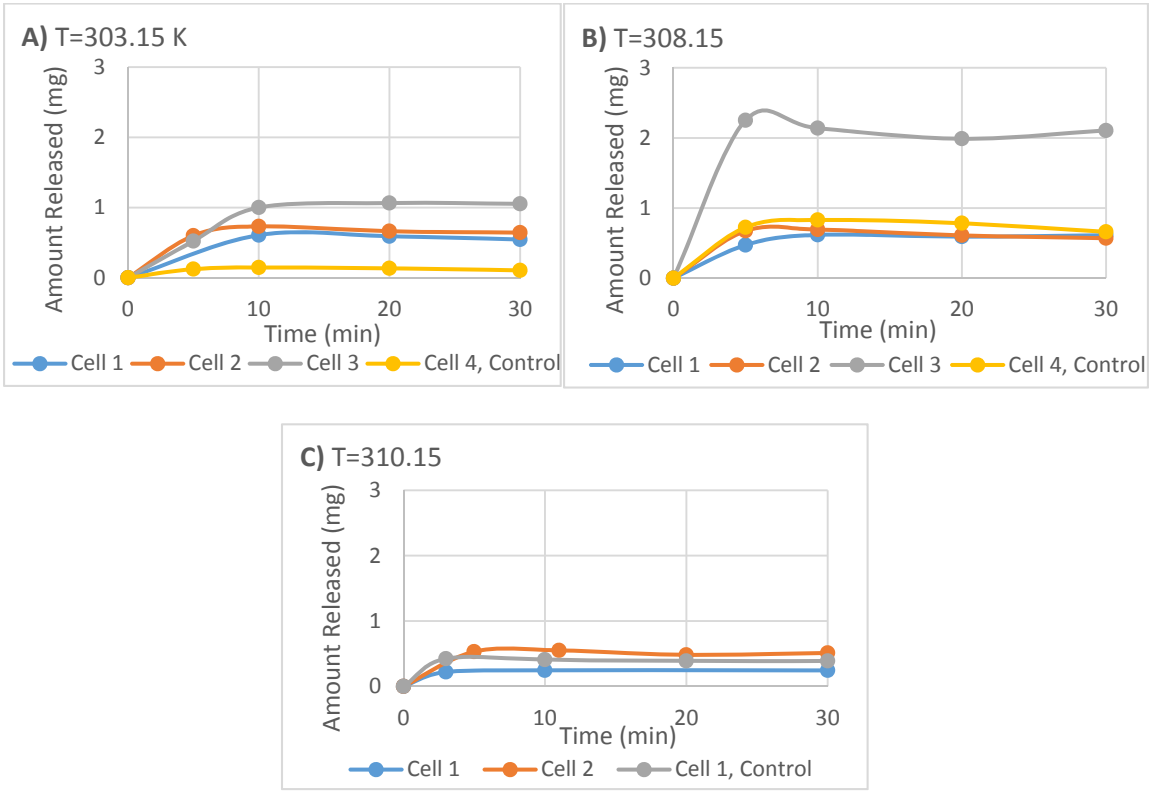

Figure 4.5 Cumulative accumulation of tetracaine with respect to time at A)30°C=303.15 K, B) 35°C=308.15 K and C) 37°C=310.15 K.

Table 4.4 Franz Cell Diffuivity Results

Temperature	Cell no.	Lidocaine Diffusivity (cm^2/s)	Tetracaine Diffusivity (cm^2/s)
30°C	1	5.50208e-07	3.68461e-09
	2	6.30504e-07	3.96706e-09
	3	9.65049e-07	5.88052e-09
	4, Control	1.87482e-07	7.84265e-10
35°C	1	9.48895e-07	5.73027e-09
	2	1.18473e-06	7.30005e-09
	3	2.70498e-06	2.648e-08
	4, Control	1.30702e-06	7.73061e-09
37°C	Cell 1	6.53372e-07	4.44946e-09
	Cell 2	6.16912e-07	5.75549e-09
	1, Control	9.8185e-07	8.57112e-09

Table 4.5 Standard Deviation Between Cell 1 and 2 Diffusivity Values and Average Drug Accumulation

	Standard Deviation of the Diffusivity		Average Maximum Accumulation (mg)	
T (°C)	Lidocaine	Tetracaine	Lidocaine	Tetracaine
30	5.67775e-08	2e-10	3.9432	0.732185
35	1.66763e-07	1.11e-09	3.5457	0.692926
37	2.57814e-08	9.24e-10	1.9292	0.530981

Table 4.4 shows that the diffusivity of lidocaine is greater than that of tetracaine by two order of magnitude, as the cell medium is aqueous. As can be seen in Table 4.5, the standard deviation between cell 1 and cell 2 is insignificant. Therefore, diffusion results for these cells may be regarded as consistent duplicates for the purpose of analysis. Comparison of the diffusivity results with respect to the control showed that the added heat enhanced diffusion below 35°C. Above this temperature, diffusivity values in the Franz Cell apparatus were not enhanced (Table 4.6). This may be attributed to the eutectic

mixture's melting point, which is 32°C. As room temperature is approximately 25°C, it is deduced that the heating components ensures that the eutectic mixture is at an optimal diffusion state, liquid, upon application of the patch. Although normal body temperature suffices to melt the eutectic mixture, the passive heat transfer would take longer without the added heating component. Furthermore, the added heat may assist in increasing skin permeability.

Table 4.6 Comparative Analysis of the Average Diffusivity of Lidocaine (top) and Tetracaine (bottom) to the Non-Oxidated Control

Lidocaine			
T (°C)	**Control Diffusivity (cm^2/s)**	**Average Diffusivity (cm^2/s)**	**% Difference**
30	1.87482E-07	5.90356E-07	68.24%
35	1.30702E-06	1.06681E-06	-22.52%
37	9.8185E-07	6.35142E-07	-54.59%

Tetracaine			
T (°C)	**Control Diffusivity (cm^2/s)**	**Average Diffusivity (cm^2/s)**	**% Difference**
30	7.84265E-10	3.82584E-09	79.50%
35	7.73061E-09	6.51516E-09	-18.66%
37	8.57112E-09	5.10248E-09	-67.98%

CHAPTER 5

CONCLUSION

The results showed that the temperature increase did not have a strong impact on the diffusive properties of lidocaine and tetracaine through the polymer membrane. Rather, the added temperature serves to facilitate better skin penetration by adjusting skin permeability and the physical state of the eutectic mixture. Further research is crucial for further specification and broadening of patch applications to include therapeutics that have charge or are larger than 500 Da. Such therapeutics include liposomal drug delivery, magnetic nanoparticle assisted drug delivery and gene therapy. Converting these treatments into TDD patches will not only alleviate the experience involved with these treatments, but it will help to improve their efficacy due to the sustained release feature of the skin patch. This pre-clinical trial, utilizing a scientific approach via computational analysis, serves as a platform for safer clinical trials.

APPENDIX A

COMPARISON OF THE CUMULATIVE ACCUMULATION WITH RESPECT TO THE DIFFUSION CONTROL

The following table shows that the difference in diffusivity is negligible above 30°C because the melting point of the eutectic mixture is 32°C. The percent difference in accumulation, with respect to the control, for lidocaine and tracaine correspond to each other. This trend is also observed in the diffusivity comparative analysis in Table 4.6.

Table A.1 Comparative Analysis of the Average Accumulation of Lidocaine (top) and Tetracaine (bottom) to the Non-Oxidated Control

Lidocaine			
T (°C)	**Control Accumulation (mg)**	**Average Accumulation (mg)**	**% Difference**
30	1.1907	3.9432	69.80%
35	4.1517	3.5457	-14.60%
37	1.6445	1.9292	14.76%

Tetracaine			
T (°C)	**Control Accumulation (mg)**	**Average Accumulation (mg)**	**% Difference**
30	0.146999883	0.732185087	79.92%
35	0.829499883	0.692925828	-16.46%
37	0.423703602	0.530981383	20.20%

REFERENCES

1. Falcone, R., Jaffe, M. and Ravindra, N.M., New screening methodology for selection of polymeric matrices for transdermal drug delivery devices, Bioinspired, Biomimetic and Nanobiomaterials, Volume 2 Issue BBN2, p. 65-75, 2013

2. FDA guideline for scale up and post approval changes (SUPAC) for in vitro release testing and in vivo, UCM 070930. Silver Spring: US Federal Drug and Admnistration, 1997, 23–28.

3. Kailas, T. D. and Chern W.H.. "Development and Validation of In Vitro Release Tests for Semisolid Dosage Forms-Case Study." *Dissolution Technol. Dissolution Technologies* 10.2 (2003): 10-15. Web.

4. Martin, S., Dressman J., Brown C. and Shah V.. "FIP/AAPS Guidelines for Dissolution/In Vitro Release Testing of Novel/Special Dosage Forms*." *Dissolution Technol. Dissolution Technologies* 10.1 (2003): 6-15. Web.

5. Raney, S. G., Lehman, P. A. and Franz, T. J. In Vitro - In Vivo Correlation (IVIVC) of Percutaneous Absorption Through Human Skin. AAPS 2010 Poster Presentation (Cetero Research). New Orleans: American Association of Pharmaceutical Scientists, 2010.

6. Marangon, A., Bock, U. and Haltner, E. http://www. acrossbarriers.de/uploads/media/FCT08_SUPAC_SS.pdf.

7. Lionberger, R. FDA Pharmaceutical Equivalence of Topical Dosage Forms Presentation. Silver Spring: US Federal Drug and Admnistration, 2005.

8. Flynn, G. L., Shah, V. P., Tenjarla, S. N., Corbo, M., DeMagistris, D., Feldman, T. G., Franz, T. J. and Miran, D. R. Assessment of value and applications of in vitro testing of topical dermatological drug products. Pharmaceutical Research 16(9), 1325.

9. Hauck, W., Shah, V.P., Shaw, S.W. and Ueda, C.T. "Reliability and Reproducibility of Vertical Diffusion Cells for Determining Release Rates from Semisolid Dosage Forms." *Pharm Res Pharmaceutical Research* 24.11 (2007): 2018-024. Web.

10. Addicks, W. J., Flynn, G. L., Weiner, N. and Chiang, C. -M. Drug Transport from thin applications of topical dosage forms: development of methodology. Pharmaceutical Research 1988, 5, 377–382.

11. Benita, S. *Submicron Emulsions in Drug Targeting and Delivery*. Amsterdam: Harwood Academic, 1998. Print.

12. "Human Skin Anatomy Diagram." *Human Anatomy Body Picture*.

13. Brannon, H., MD. "Stratum Corneum Anatomy - The Key to Healthy, Attractive Skin." *About.com Health*. 4 Nov. 2009. Web. <http://dermatology.about.com/od/anatomy/ss/sc_anatomy.htm>.

14. Bos, J.D., Marcus, M.H. and Meinardi M.. "The 500 Dalton Rule for the Skin Penetration of Chemical Compounds and Drugs." *Experimental Dermatology Exp Dermatol* 9.3 (2000): 165-69.

15. Pond, S.M., and Tozer T.N.. "First-Pass Elimination." *Clinical Pharmacokinetics* 9.1 (1984): 1-25. Web.

16. Gagliardi, M.. *Global Markets and Technologies for Thin-Film Batteries*. Rep. no. FCB036A. *BCC Research*. Aug. 2013. Web. <http://www.bccresearch.com/market-research/fuel-cell-and-battery-technologies/thin-film-batteries-fcb036a.html> Executive Summary

17. Bhowmik, D., Duraivel, S. and Sampath Kumar, K.P. "Recent Trends in Challenges and Opportunities in Transdermal Drug Delivery System." *The Pharma Innovation* 1.10 (2012): 9-23. Web. <http://www.thepharmajournal.com/vol1Issue10/Issue_dec_2012/2.1.pdf>

18. Sampath Kumar, K.P., Bhowmik, D., Chiranjib, B. and Chandira, R. M. "Transdermal Drug Delivery System - A Novel Drug Delivery System and Its Market Scope and Opportunities." *International Journal of Pharma and Bio Sciences* 1.2 (2010): 1-21. Web.

19. Bolognia J., Jorizzo, J.L. and Schaffer, J.V. *Dermatology*. 3rd ed. Vol. 1. Philadelphia: Elsevier Saunders, 2012. Section 19. Print http://drugdelivery.chbe.gatech.edu/Papers/2012/Prausnitz%20Derm%20Book%20Chapter%202012.pdf

20. Pond, S.M. and Tozer, T.N. "First-Pass Elimination." *Clinical Pharmacokinetics* 9.1 (1984): 1-25. Web.

21. "First Pass and Plasma Drug Levels (Introduction) (Human Drug Metabolism)." *Whatwhenhow RSS*. Web. 03 Feb. 2016.

22. Paudel, K.S., Milewski, M., Swadley, C.L., Brogden, N.K., Ghosh, P. and Stinchcomb, A. L. "Challenges and Opportunities in Dermal/transdermal Delivery." *Therapeutic Delivery* 1.1 (2010): 109-31.

23. Margetts, L. and Sawyer, R. "Transdermal Drug Delivery: Principles and Opioid Therapy." *Contin Educ Anaesth Crit Care Pain Continuing Education in Anaesthesia, Critical Care & Pain* 7.5 (2007): 171-76. Web.

24. Crank, J., *The Mathematics of Diffusion*. 2nd ed. Oxford: Clarendon, 1975, 1-14.

25. Stein, W.D. and Lieb, W. R.. *Transport and Diffusion across Cell Membranes*. Orlando: Academic, 1986, 94-102.

26. "Joback Method." *Project Gutenberg Self-Publishing Portal*. World Heritage Encyclopedia. Web. <http://central.gutenberg.org/articles/Joback_method>.

27. Bondi, A. "Free Volumes and Free Rotation in Simple Liquids and Liquid Saturated Hydrocarbons." *The Journal of Physical Chemistry J. Phys. Chem.* 58.11 (1954): 929-39.

28. Naik, A., Kalia, Y.N. and Guy, R.H. "Transdermal Drug Delivery: Overcoming the Skin's Barrier Function." *Pharmaceutical Science & Technology Today* 3.9 (2000): 318-26. Web.

29. Rawat, S., Vengurlekar, S., Rakesh, B., Jain, S. and Srikarti, G. "Transdermal Delivery by Iontophoresis." *Indian Journal of Pharmaceutical Sciences Indian J Pharm Sci* 70.1 (2008): 5. Print.

30. Binghe, W., Hu, L. and Siahaan, T.. *Drug Delivery: Principles and Applications*. Print.

31. Lee, J.W., Priya, G., Park, J.H., Allen, M.G. and Prausnitz, M.R. "Microsecond Thermal Ablation of Skin for Transdermal Drug Delivery." *Journal of Controlled Release* 154.1 (2011): 58-68. Web.

32. Vizserálek, G., Tamás, B., Takács-Novák, K. and Sinkó, B. "PAMPA Study of the Temperature Effect on Permeability." *European Journal of Pharmaceutical Sciences* 53 (2014): 45-49. Print.

33. Deveaugh-Geiss, A.M., Chen, L.H., Kotler, M.L., Ramsay, L.R., and Durcan M.J. "Pharmacokinetic Comparison of Two Nicotine Transdermal Systems, a 21-mg/24-hour Patch and a 25-mg/16-hour Patch: A Randomized, Open-label, Single-dose, Two-way Crossover Study in Adult Smokers." *Clinical Therapeutics* 32.6 (2010): 1140-148.

34. Tonge, M.P. and Gilbert, R.G. "Testing Models for Penetrant Diffusion in Glassy Polymers." *Polymer* 42.2 (2001): 501-13. Web.

35. Yamada, T. and Gunn, R.D.. "Saturated Liquid Molar Volumes. Rackett Equation." *Journal of Chemical & Engineering Data J. Chem. Eng. Data* 18.2 (1973): 234-36. Web.

36. Mendieta-Taboada, O., Sobral, P.J., Carvalho, R.A. and Habitante, A.M.B. "Thermomechanical Properties of Biodegradable Films Based on Blends of Gelatin and Poly(vinyl Alcohol)." *Food Hydrocolloids* 22.8 (2008): 1485-492. Web.

37. Camacho-Zuñiga, C. and Ruiz-Treviño, F.A. "A New Group Contribution Scheme To Estimate the Glass Transition Temperature for Polymers and Diluents." *Industrial & Engineering Chemistry Research Ind. Eng. Chem. Res.* 42.7 (2003): 1530-534. Web.

38. "Poly(vinylalcohol)." *Polymer Data Base*. 2015. Web. <http://polymerdatabase.com/polymers/polyvinylalcohol.html>

39. Pitzer, K.S. "The Volumetric and Thermodynamic Properties of Fluids. I. Theoretical Basis and Virial Coefficients 1." *J. Am. Chem. Soc. Journal of the American Chemical Society* 77.13 (1955): 3427-433. Web.

40. Kumar, B. K., Rajan, V. and Begum, N.T. "Analytical Method Development and Validation of Lidocaine in Ointment Formulation by U.V Spectrophotometric Method." *International Journal of Pharmacy and Pharmaceutical Sciences* 4.2 (2012): 610-14. Web.

41. Bempong, D. K. "USP Monographs: Tetracaine." *USP Monographs: Tetracaine*. US Pharmacopeia. <http://www.pharmacopeia.cn/v29240/usp29nf24s0_m81550.html>

42. Ng, S.F., Rouse, J.J., Sanderson, F.D., Meidan, V. and Eccleston, G.M. "Validation of a Static Franz Diffusion Cell System for In Vitro Permeation Studies." *AAPS PharmSciTech* 11.3 (2010): 1432-441. Web.

43. Galen Pharmaceuticals. *Synera (Lidocaine and Tetracaine) Topical Patch Prescribing Information*. Souderton, PA: Galen Pharmaceuticals, 2013. Print.